

INAUGURAL-DISSERTATION

zur
Erlangung der Doktorwürde
der
Fakultät für Pharmazie
der
Ruprecht-Karls-Universität
Heidelberg

vorgelegt von

Diplom-Chemiker Ragen Pfeiffer

aus Berlin

Tag der mündlichen Prüfung: 17.12.2001

Development of Methods to Investigate Poly(ADP-ribose) polymerase-1 activity and DNA Base-Excision Repair in Relation to Cancer and Ageing

Erstgutachter:

Prof. Dr. Manfred Wießler

Zweitgutachter:

Priv.-Doz. Dr. Alexander Bürkle, Senior Lecturer

Contents

	<i>page</i>
Abbreviations	5
I. Introduction	6
I. 1. Poly(ADP-ribose) polymerase-1	6
I. 2. Homologues of PARP-1	8
I. 3. Physiological and pathophysiological functions of PARP-1	9
I. 4. DNA excision repair in mammalian cells	11
I. 5. The mechanism of base-excision repair and the involvement of PARP-1	13
I. 6. The involvement of DNA repair and PARP-1 in the ageing process	17
I. 7. Current methods to detect and quantify poly(ADP-ribose)	21
I. 8. Current methods to measure DNA damage and DNA repair	24
I. 9. Aim of the project	28
II. Materials	31
II. 1. Appliances	31
II. 2. Chemicals	33
II. 3. Oligonucleotides	33
II. 4. Antibodies	34
II. 5. Membranes	34
II. 6. Buffers and solutions	34
II. 7. Cell culture medium	35
II. 8. Cell lines	35
II. 9. Animals and human blood donors	35
III. Methods	37
III. 1. Poly(ADP-ribose) immuno-dot-blot assay	37
III. 2. Automated fluorescence-detected alkaline DNA unwinding assay	38

IV. Results	40
IV. 1. Setting up a new immuno-dot-blot procedure to assess cellular poly(ADP-ribosyl)ation capacity.	40
IV. 2. Evaluation of the new poly(ADP-ribose) immuno-dot-blot assay	44
IV. 3. Setting up an automated version of the fluorescence-detected alkaline unwinding (FADU) assay to quantify DNA strand breaks and repair in live cells.	46
IV. 4. Comparison of DNA strand break repair in a long-lived (human) and a short-lived (rat)mammalian species.	54
IV. 5. Comparison of DNA strand break repair in PARP-1 ^{-/-} and PARP-1 ^{+/+} cells.	57
V. Discussion	59
VI. Summary	63
VII. References	65
VIII. Own publications	73
IX. Acknowledgements	75

Abbreviations

b	base
bp	base pair
BER	base-excision repair
β -MeEtOH	β -mercaptoethanol
DMSO	dimethylsulfoxid
Ex	excitation
Em	emission
ECL+	enhanced chemoluminescence+
EDTA	ethylenediaminetetraacetate
FADU	fluorescence-detected alkaline DNA unwinding
Gy	Gray
EtBr	ethidium bromide
FcS	foetal calf serum
MNC	mononuclear cells
MMR	mismatch repair
MNU	N-methyl-N-nitrosourea
NER	nucleotide-excision repair
NLS	nuclear location signal
p(ADP)r	poly(ADP-ribose)
PARP-1	poly(ADP-ribose) polymerase-1; (EC 2.4.2.30)
ROI	reactive oxygen intermediates
SDS	sodium dodecylsulfate
TCA	trichloroacetic acid
TEMED	N,N,N',N'-tetramethylethylenediamine
Tris	Tris(hydroxymethyl)aminomethane
VPARP	Vault-associated poly(ADP-ribose) polymerase

I. Introduction

I. 1. Poly(ADP-ribose) polymerase-1

Catalytic activation of poly(ADP-ribose) polymerase-1 (PARP-1; EC 2.4.2.30) is one of the immediate early reactions of eukaryotic cells to DNA-damaging treatment (for review: de Murcia & Shall, 2000; Bürkle, 2001a,b). PARP-1 is a nuclear 113-kDa enzyme that consists of three domains (Fig. 1.): (1) A DNA-binding domain with two Zn²⁺ finger motifs (Gradwohl et al., 1990) and a nuclear location signal (NLS) (Schreiber et al., 1992); (2) an automodification domain, which serves as the major site for covalent attachment of (ADP-ribose) polymer; and (3) an NAD⁺-binding domain comprising the catalytic centre.

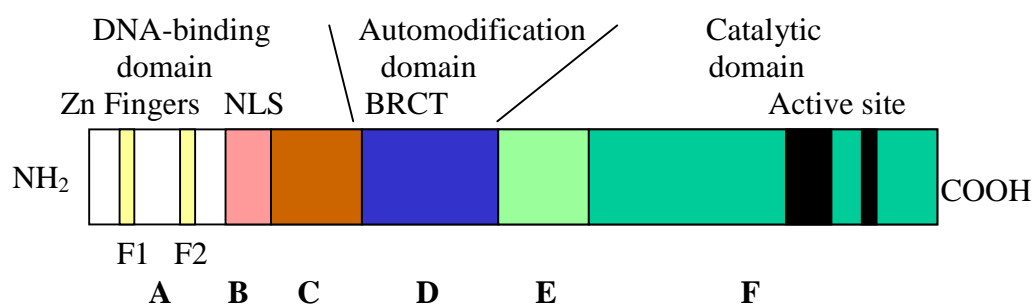


Fig. 1. Domain structure of PARP-1. The 113-kDa enzyme possesses at its N-terminal DNA binding domain two Zn fingers (F1 and F2)[module A] as well as a nuclear location signal (NLS) [module B] that consists of two parts. In between these two parts there is a caspase-3 cleavage site. The second domain is the automodification domain [module D]. The third and C-terminal domain [modules E and F] carries the active site. Modified from de Murcia & Shall, 2000.

PARP-1 is a nuclear protein of very high abundance, with 500.000 to one million copies per cell (Ludwig et al., 1988), but is absent from the cytoplasm. PARP-1 activation is one of the first cellular responses to exposure to genotoxic agents.

PARP-1 specifically recognises DNA single and double-strand breaks via its zinc-fingers. The first zinc-finger binds to double-strand breaks, whereas the second zinc-finger is specific for single-strand breaks (de Murcia & Shall, 2000). However, the first zinc-finger is essential for the catalytic activity of PARP-1 by both double and by single strand breaks (Ikejima et al., 1990). PARP-1 is acting as a catalytic dimer (Mendoza-Alvarez & Alvarez-Gonzales, 1993), *i.e.* two PARP-1 molecules are binding to one strand break, with one enzyme molecule

serving as the catalyst and the other as “acceptor” protein (*i.e.* substrate). On either side of the strand break 7 nucleotides are involved in the DNA-PARP-1 interaction and the typical V-shape of nicked DNA is stabilised (LeCam et al., 1994). The binding is very specific and of high affinity and leads to a 500-fold enhancement of the activity of the catalytic centre, probably mediated by some as yet unknown conformational change. Fig. 2 depicts the chemical structure of poly(ADP-ribose) [p(ADPr)], which is a biopolymer characterised by unique O-glycosidic ribose-ribose bonds (Chambon et al., 1966).

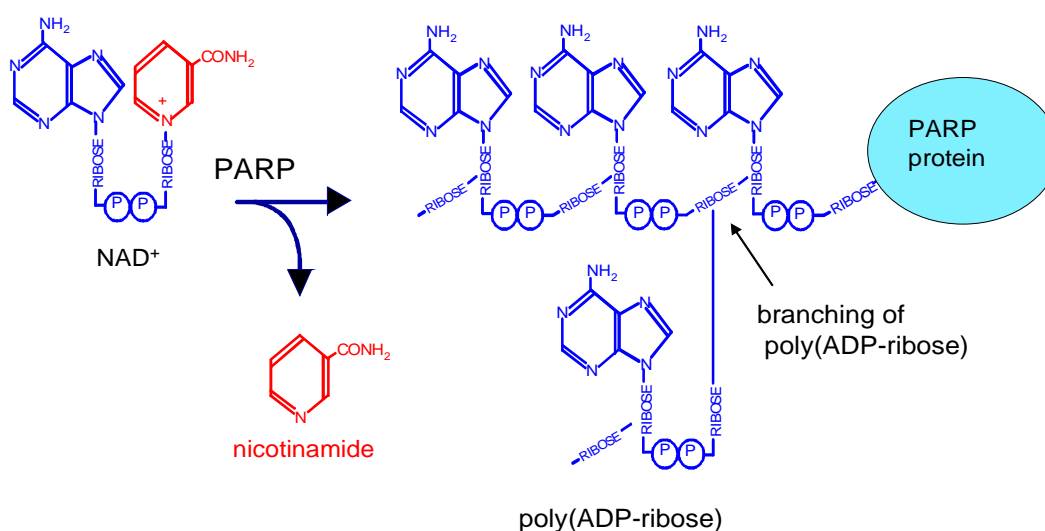


Fig. 2. Chemical structure of poly(ADP-ribose). PARP-1 splits β -NAD⁺ thus releasing nicotinamide. The ADP-ribosyl units are covalently linked to each other via α -glycosidic bonds to form the polymer.

The substrate for polymer formation is β -NAD⁺. Nicotinamide is released from β -NAD⁺ and the resulting ADP-ribosyl moiety is used to form ADP-ribose polymer (Althaus and Richter, 1987). Polymerisation starts with the formation of an ester bond between the first ADP-ribose unit with a glutamate or aspartate residue of an acceptor protein (mostly PARP-1 itself). During the elongation reaction up to 200 additional ADP-ribose units can be added via formation of unique 1''-2'-O-glycosidic bonds between the 2' carbon atom of the adenine-proximal ribose of an already coupled ADP-ribose unit and the 1'' carbon of the adenine-distal ribose of a new ADP-ribose unit. Branching of the polymer occurs at around every 40th

unit by linking two adenine-distal ribose moieties. Electrostatic repulsion of PARP-1 from DNA via the highly negatively charged polymer causes the termination of the polymerisation (Durkacz et al., 1980). The polymer may then attract various repair enzymes and/or removes histones from the DNA (Naegeli and Althaus, 1992), thus orchestrating the sequential steps in DNA base-excision repair.

Degradation of the ADP-ribose polymer is carried out by p(ADPr) glycohydrolase, which rapidly splits the polymer into eicosamers. These are then degraded into monomers at a lower rate (Braun et al., 1994).

Orthologues of PARP-1 can be found in most eukaryotes, but not in yeast nor in prokaryotes. The primary structure of PARP-1 in mammals is highly conserved, as revealed by sequence comparisons of mouse (Huppi et al., 1989), rat (Beneke et al., 1997), cow (Saito et al., 1990), and human (van Gool et al., 1997) PARP-1 cDNA. Between the human and mouse PARP-1 the overall homology is 92 % at the amino acid level, and the homology of the catalytic site is 100 %.

I. 2. Homologues of PARP-1

It was found that cells from PARP-1^{-/-} mice surprisingly do possess some residual p(ADPr) formation activity (Shieh et al., 1998). This finding triggered the discovery of a number of homologues of the PARP-1, encoded by separate genes. The current knowledge about the new members of the “PARP family” can be summarised as follows.

The 65-kDa PARP-2 enzyme is activated by DNA damage, as has long been known for PARP-1, but surprisingly is devoid of any zinc finger motif and the molecular basis for its DNA binding is not understood. Its function is most closely related to that of PARP-1. The phenotype of PARP-2^{-/-} mice is very similar to PARP-1^{-/-} mice *i.e.*, mice are viable and fertile but hypersensitive to ionising radiation or alkylating agents. Double knockout mice are not viable. PARP-2 probably functions as a back-up enzyme for PARP-1 with respect to DNA repair and the maintenance of genomic stability under normal conditions, even though no up-regulation of the PARP-2 gene could be found in PARP-1^{-/-} cells (Amé et al., 1999).

PARP-3, a 60-kDa protein, does not possess any DNA-binding site at all (Johansson, 1999). Its function is totally unknown.

The 193-kDa PARP-4, also called VPARP (V standing for Vault), was found to be one of the three proteins present in Vault-particles (Jean et al., 1999; Kickhoefer et al., 1999). The function of Vault-particles still remains unclear. They may perhaps play a role in intracellular transport. VPARP is interacting with the mitotic spindle microtubules in HeLa cells, suggesting a role for this enzyme at the end of cellular division.

Tankyrase (PARP-5) is a 142-kDa protein containing 26 ankyrin repeats and a PARP catalytic fragment of limited size (Smith et al., 1998). It has been localised to human telomeres. Tankyrase can poly(ADP-ribosyl)ate the telomere-binding protein TRF1 (de Lange, 1998 and van Steensel and de Lange, 1997). TRF1 then loses its affinity to DNA. It is possible that Tankyrase plays an important role in the regulation of human telomeres.

I. 3. Physiological and pathophysiological functions of PARP-1

PARP-1^{-/-} mice show impaired DNA repair after N-methyl-N-nitrosourea (MNU) treatment, as determined by the alkaline comet assay (Trucco et al, 1998). MNU is an agent that introduces damage into the DNA that is mostly repaired by the DNA base-excision repair (BER) pathway. In addition PARP-1 has been found to have a binding site to XRCC1, which seems to play a crucial role in the BER pathway (Masson et al, 1998). More detail is provided in Fig. 4. In this context, it is interesting to note that PARP-1^{-/-} mice have a largely normal phenotype and do not show a higher incidence of spontaneous tumours. However, if exposed to genotoxic agents the formation of cancer is enhanced (Tsutsumi et al, 2001).

A strong, positive correlation between maximal life span of mammals and maximal PARP-1 activity in permeabilised mononuclear blood cells has been established (Pero et al., 1985; Grube & Bürkle, 1992). Furthermore, in permeabilised lymphoblastoid cell cultures derived from centenarians higher maximal PARP-1 activity was observed than in controls (Muiras et al., 1998). How PARP-1 may possibly be involved in the ageing process is illustrated below in Figs. 6 and 7.

Meyer et al. (2000) have shown that DNA damage-induced sister-chromatid exchange is inhibited if PARP-1 is overexpressed. These and other results implicate that PARP-1 plays an active role in the maintenance of genomic stability in cells under genotoxic stress (Bürkle, 2001c).

Tumour cells treated with chemotherapy or radiotherapy often are selected to become resistant against the treatment. Few resistant cells, which survive an initial treatment, are then able to grow up to a drug-resistant untreatable new tumour mass. Reducing the mutability of cancer cells via overexpressing PARP-1 might therefore slow down the emergence of resistant tumour cells, yielding fewer or no resistant cells escaping the initial treatments. New therapies against cancer might be possible using viral vectors transducing the PARP-1 gene.

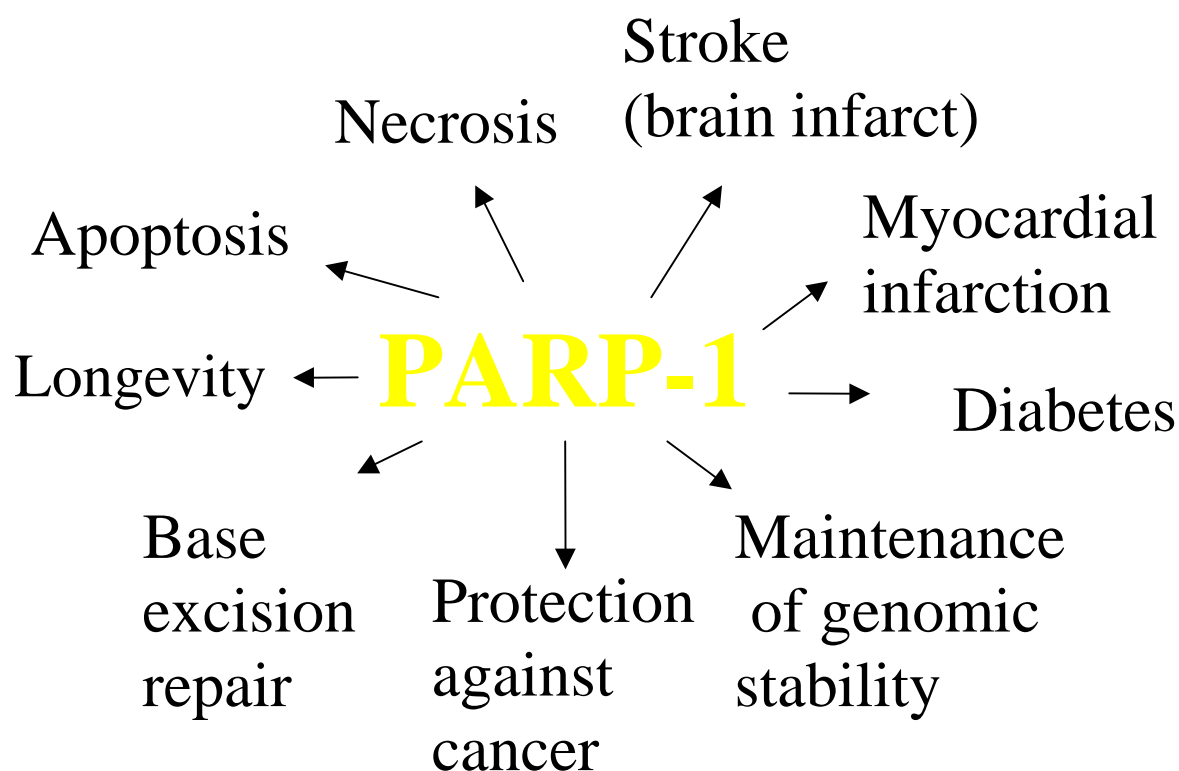


Fig. 3. Involvement of PARP-1 in diverse biological processes. PARP-1 seems to be involved in a variety of important physiological and pathological processes, such as DNA base-excision repair, maintenance of genomic stability of cells under genotoxic stress, longevity assurance, protection from cancer formation, cell death, type-1 diabetes, and tissue infarction. For details see text.

If severe DNA damage is inflicted to cells, there can be massive activation of PARP-1. This may cause a depletion of cellular NAD^+ pools. As a consequence large amounts of cellular ATP will then be needed for *de-novo* synthesis of NAD^+ . At the same time, a severe NAD^+ depletion will inhibit both glycolysis and respiration, leading to a complete energy depletion of the cell. There is no possibility for a cell to recover from such a situation and the cell is bound to die of necrosis (Berger, 1985). This scenario has been confirmed in a number of pathophysiological conditions. For instance, experimentally induced ischemia-reperfusion in brain, which serves as a model for stroke, is associated with massive release of endogenous

DNA-damaging compounds, including ROI, and leads to brain infarct. It has been shown that abrogation of PARP-1 activity, either by PARP-1 gene disruption or administration of low-molecular weight inhibitors, leads to an increased survival of the neurones at risk and dramatic reduction of brain infarct size (Eliasson et al., 1997). Very similar effects of PARP-1 inhibition on NO-induced necrosis have been observed in pancreatic islet cells (Radons et al., 1995). These data as well as other data obtained in different organs clearly indicate that PARP-1 is involved in the pathogenesis of tissue infarcts in heart and brain and of juvenile diabetes (type 1). Therefore new therapies might arise based on the use of specific PARP-1 inhibitors.

During apoptosis PARP-1 is cleaved by caspase-3 in the NLS region into two defined fragments of 24 kDa (N-terminal) and 89 kDa (C-terminal). This PARP-1 cleavage is widely used as a specific marker for apoptosis (Kaufmann et al., 1993, Alvarez-Gonzalez et al., 1999) and might also serve as a clinical diagnostic tool, *e.g.* in cancer treatment.

I. 4. DNA excision repair in mammalian cells

In mammalian cells DNA excision repair consists of three major pathways: base-excision repair (BER), nucleotide-excision repair (NER) and mismatch repair (MMR). Several other repair pathways that have been detected in lower eukaryotes or in prokaryotes apparently do not exist in mammals. One might speculate that only very reliable forms of DNA repair, which make very few errors, proved suitable for animals with very long life spans, and thus unreliable, mutation-prone pathways of DNA repair were lost during evolution.

The first step in BER is the excision of a single base carrying a lesion. Then the sugar-phosphate backbone is opened and the residual sugar-phosphate moiety is removed. In addition a varying number of nucleotides can be removed as well (for a more detailed description, see below). Typical lesions which are repaired by BER are “small” alterations of bases (*e.g.* oxidation, alkylation). Oxidation is mediated by oxygen free radicals, which arise both from various endogenous processes such as mitochondrial respiration, and from exposure to exogenous chemicals such as peroxides or bleomycin, or physical agents such as γ -radiation (see below). Another substrate for BER are abasic sites directly arising from spontaneous hydrolysis of the glycosidic bond connecting the base with C1' of deoxyribose.

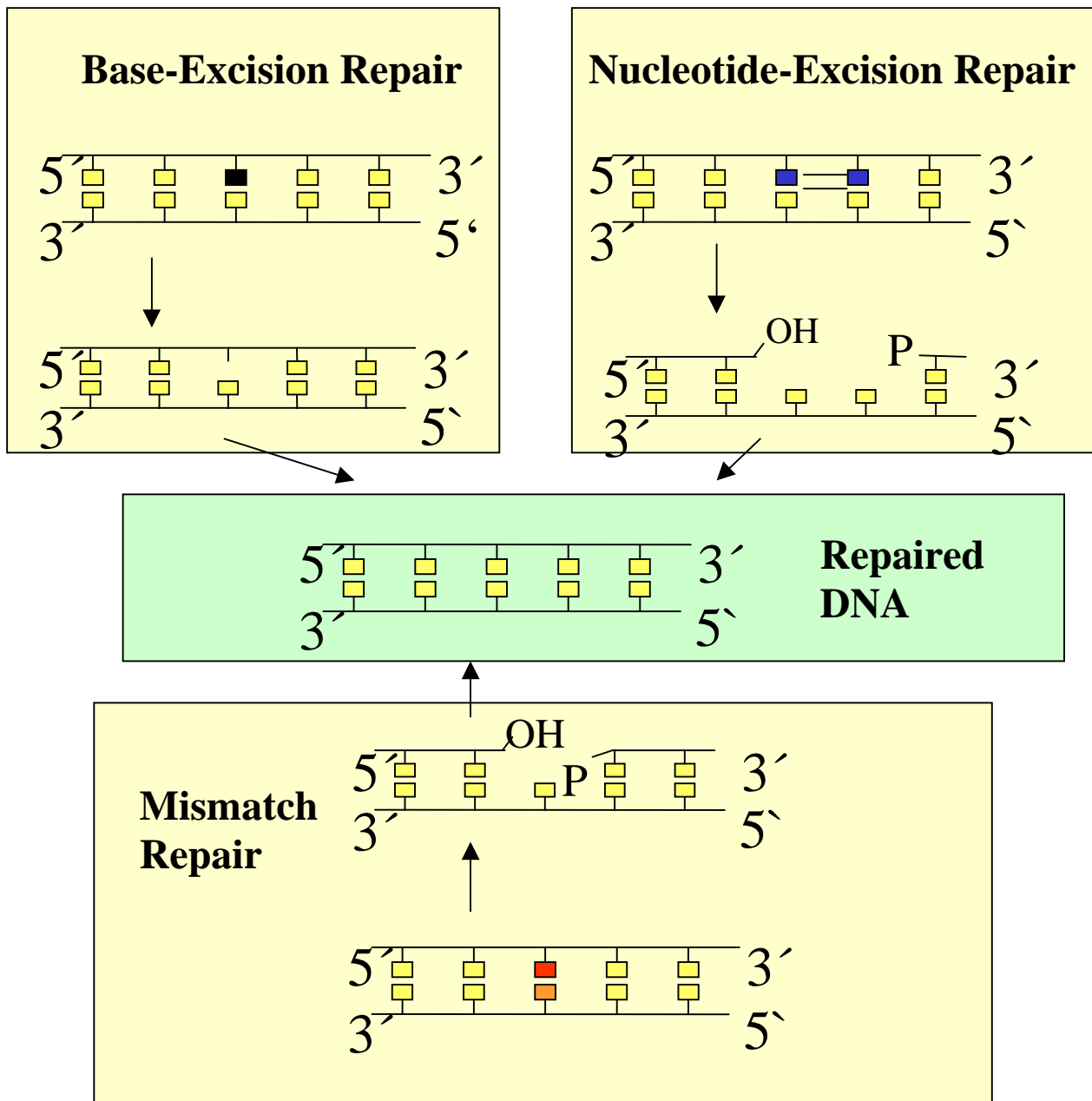


Fig. 4. Major functional differences between the three major DNA excision repair pathways in mammalian cells. In base excision repair the altered base is first excised without breakage of the sugar-phosphate backbone. Only subsequently is the sugar-phosphate backbone opened, the rest of the nucleotide removed and the missing nucleotide replaced. For more detail see Fig. 5. The function of mismatch repair is identification and correction of mismatched bases, mostly introduced as DNA replication errors. Typically, large segments (up to several kilobases) of the strand carrying the misincorporated base are excised followed by resynthesis using the cells DNA replication machinery. In nucleotide excision repair oligonucleotides of about 30 nucleotides, incorporating the lesion site, are cut out followed by resynthesis.

γ -Radiation can damage DNA either via direct energy transfer to this macromolecule or via radiolysis of water, leading to formation of ROI causing oxidative damage. The wide spectrum of radiation-induced lesions ranges from damaged bases or deoxyribose moieties to direct formation of DNA single and double strand breaks. All of these can be repaired via base excision repair, except double strand breaks, which require repair via “non-homologous end joining” (NHEJ) or recombination pathways. It should be noted that unrepaired double strand breaks are extremely cytotoxic lesions, with a single break of this kind being sufficient to induce apoptosis.

NER is characterised by the excision of an oligonucleotide from damaged DNA as an initial step. Typical kinds of damage that will be removed by nucleotide excision repair are pyrimidine photodimers and other photoproducts caused by UV-B and UV-C radiation, as well as “bulky” chemical adducts, induced for instance by polycyclic aromatic hydrocarbons (*e.g.* benzo[a]pyrene), and DNA crosslinks. NER has its own set of enzymes operating at any stage of the process.

MMR is defined by the kind of damage introduced into DNA rather than by the pathway of the repair. Typical kinds of “damage” to be recognised by the MMR machinery are mismatching pairs of normal bases resulting from misincorporation of nucleotides during normal DNA synthesis or base pair mismatches induced by alkylation of one partner (*e.g.* O⁶-methylguanine formation). Different sub-pathways exist, which have their individual sets of enzymes.

I. 5. The mechanism of base-excision repair and the involvement of PARP-1

The first step of BER is recognition of a damaged base by a DNA base glycosylase and base removal without breaking the sugar-phosphate backbone. In mammals there exist a whole variety of glycosylases, all of which recognise and remove bases that carry specific kinds of lesions from DNA. As mentioned above, there is yet another mechanism of abasic site formation, *i.e.* spontaneous hydrolysis of the relatively weak glycosidic bond linking the base with the sugar-phosphate backbone of the DNA.

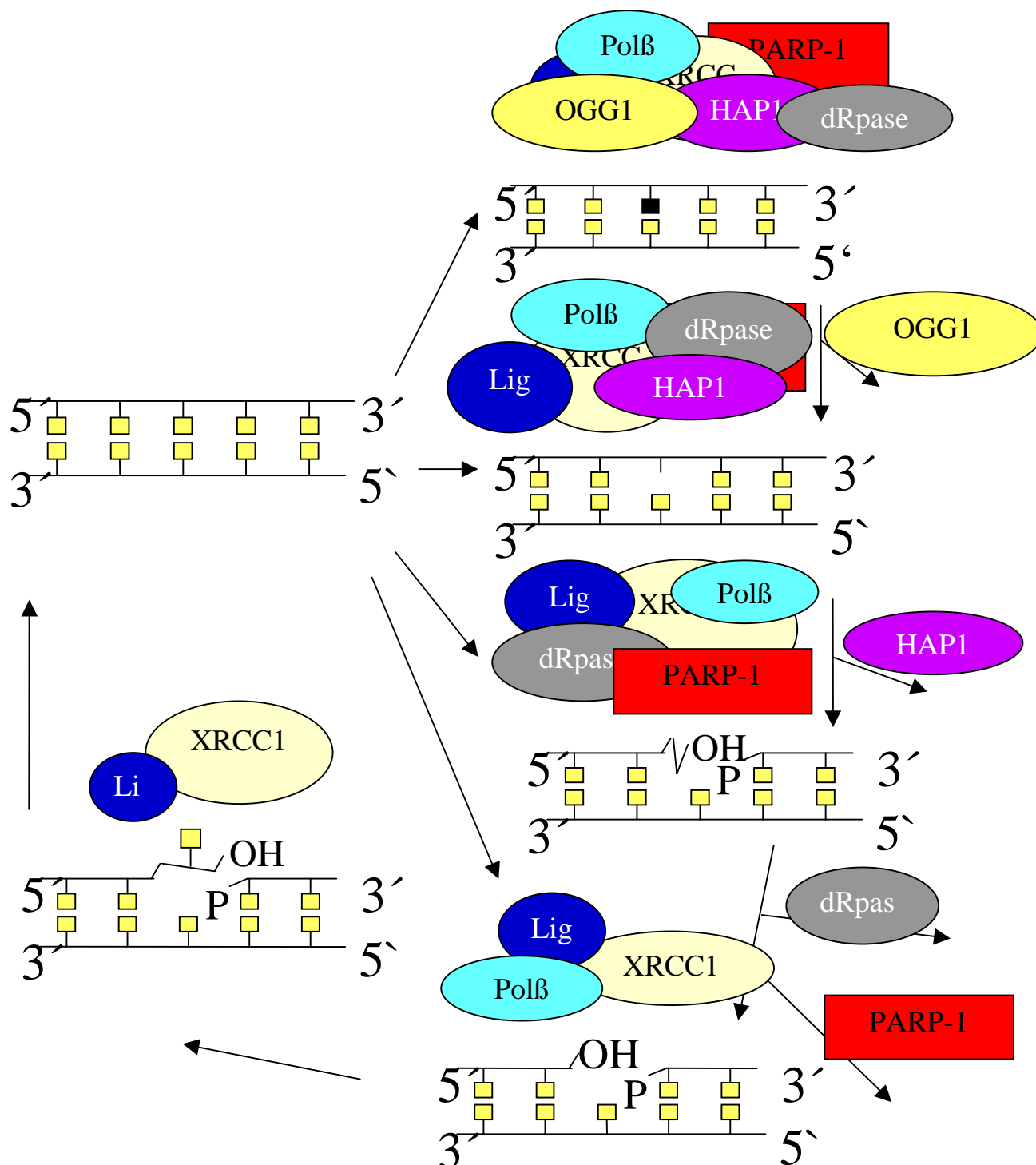


Fig. 5. Scheme of the DNA base-excision repair pathway and the key enzymes involved. Different kinds of damaging agents can cause different kinds of damages, which can enter the base-excision repair pathway at different stages. Chemical alterations of DNA bases, such as oxidation or alkylation, will be recognised by DNA glycosylases, one of which is OGG1. Glycosylase activity then generates an apurinic / apyrimidinic (AP) site.

It is important to note that even in the absence of base damage, DNA can undergo spontaneous hydrolysis of the N-glycosidic bonds linking the bases with the deoxyribose, resulting in direct formation of AP sites.

AP sites are recognised by an AP endonuclease (e.g. HAP1), catalysing hydrolysis of the phosphodiester bond. This results in 5' terminal deoxyribose-phosphate moiety, which is then excised by a DNA deoxyribose phosphodiesterase (dRpase).

At this stage PARP-1 binds to the strand break and gets automodified with p(ADPr). It is thought that automodified PARP-1 can cause local relaxation of chromatin, due to the extremely high affinity, by which histones bind to p(ADPr).

As a next step, DNA polymerase β (Pol β) fits in the missing nucleotide and ligation by ligase I or III (Lig) takes place.

γ -Radiation leads to several different kinds of damage that can be removed by DNA BER, including damage to bases or deoxyribose moieties as well as direct formation of DNA single strand breaks. By contrast, double strand breaks, which can also arise as a direct result of γ irradiation, are not a substrate for BER, but have to be repaired via “non-homologous end joining” (NHEJ) or recombination pathways rather.

As a next step the residual sugar-phosphate moiety is cut out by AP endonuclease (HAP1) leaving a gap of just one nucleotide. This is followed by DNA repair synthesis, which is either of the “short patch” type, representing the major pathway and filling in only one nucleotide, or “long patch” type, filling in 2-6 nucleotides.

As a next step PARP-1 binds to the DNA strand break and gets automodified with ADP-ribose polymer. The precise function of PARP-1 at the molecular level in this process remains elusive. It has been shown that PARP-1 is able to interact with DNA polymerase- β but not with DNA polymerases δ or ϵ (Dantzer et al., 2000). DNA polymerase- β has been shown to be involved in both long patch and short patch BER (Klungland and Lindahl, 1997; Dianov et al., 1999). In the absence of both PARP-1 and DNA-polymerase- β BER is extremely inefficient and one may speculate on a functional synergy between the two proteins (Dianov et al., 1999).

There is apparently not just a single function PARP-1 has to fulfil in BER. PARP-1 has been shown to interact with the tumour suppressor protein p53, thus perhaps playing a role in signalling DNA damage to cell-cycle checkpoint proteins and influence the decision of whether or not to progress in cell cycle (Trucco et al., 1998) or even to trigger the apoptotic programme in the presence of massive DNA damage.

There is substantial evidence that PARP-1 plays a role in chromatin remodelling either via covalently modifying histones (de Murcia et al., 1988; de Murcia et al., 1986) and/or via histones binding non-covalently to p(ADPr) automodifying PARP-1 (Althaus et al., 1994). The resulting local and reversible decondensation of DNA could facilitate the DNA repair process.

DNA polymerase- β fills in the missing nucleotides, and the function of ligases I or III is finally to covalently close the interrupted DNA strand.

XRCC1 can be viewed as an organising or “scaffolding” protein. It is present throughout the whole BER process, having binding sites for nicked DNA itself and for most proteins involved in the base excision repair process like PARP-1, OGG1, DNA polymerase- β and ligase III.

I. 6. The involvement of DNA repair and PARP-1 in the ageing process

One of the central predictions of the Disposable Soma Theory of ageing (Kirkwood, 1977; Kirkwood & Austad 2000) is that critical limitations exist in macromolecular maintenance and repair of somatic cells. Such limitations are thought to have evolved in accordance with the extrinsic mortality level an animal species is facing in a given habitat, as a result of a trade-off between allocating of available bioenergy to somatic maintenance and repair on the one hand and reproducing as well as other energy-consuming activities (*e.g.* muscular activity) on the other. Given the constant attack of biological macromolecules by endogenous and exogenous damaging compounds such as ROI, it is thought that somatic maintenance and repair act as critical determinants of cellular stress resistance and organismal longevity.

Specifically, in the adult body one may group the cells in two different classes, *i.e.* cells that are post-mitotic and have stopped dividing, and cells that are proliferative. Examples for the first group are muscle cells, neurones and cells that form the eye lens. Most neurones of the body are generated during the embryonic and foetal phase of development and will persist for the rest of the body's lifetime, although in some regions of the brain, stem cells have recently been identified from which new neurones can arise as a replacement of single degenerated neurones, but not of those lost in larger numbers as a result of brain trauma or disease processes. Likewise, most of post-natal striated muscle fibres are thought to persist throughout lifetime, although there is seemingly some regenerative potential provided by muscle stem cells. Terminally differentiated cells of the eye lens even lose most of their organelles and to become transparent. The potential problems arising from ageing in such cells that may persist for many decades if not a century are very different from those in proliferating cells (Fig. 6.). Cancer formation is extremely rare in postmitotic cell types. Instead there is the problem of waste products accumulating over time, like lipofuscin, and of accumulation of mitochondrial DNA mutations, ultimately leading to severe deficiency in bioenergy metabolism, which cause the characteristic problems in these cells. Another major problem for post-mitotic cells might be represented in cascades of deteriorating information-storage or information-transmitting molecules, leading to error accumulation at all levels of the metabolic machinery of the cell (Fig. 6) and finally functional impairment and even cell death.

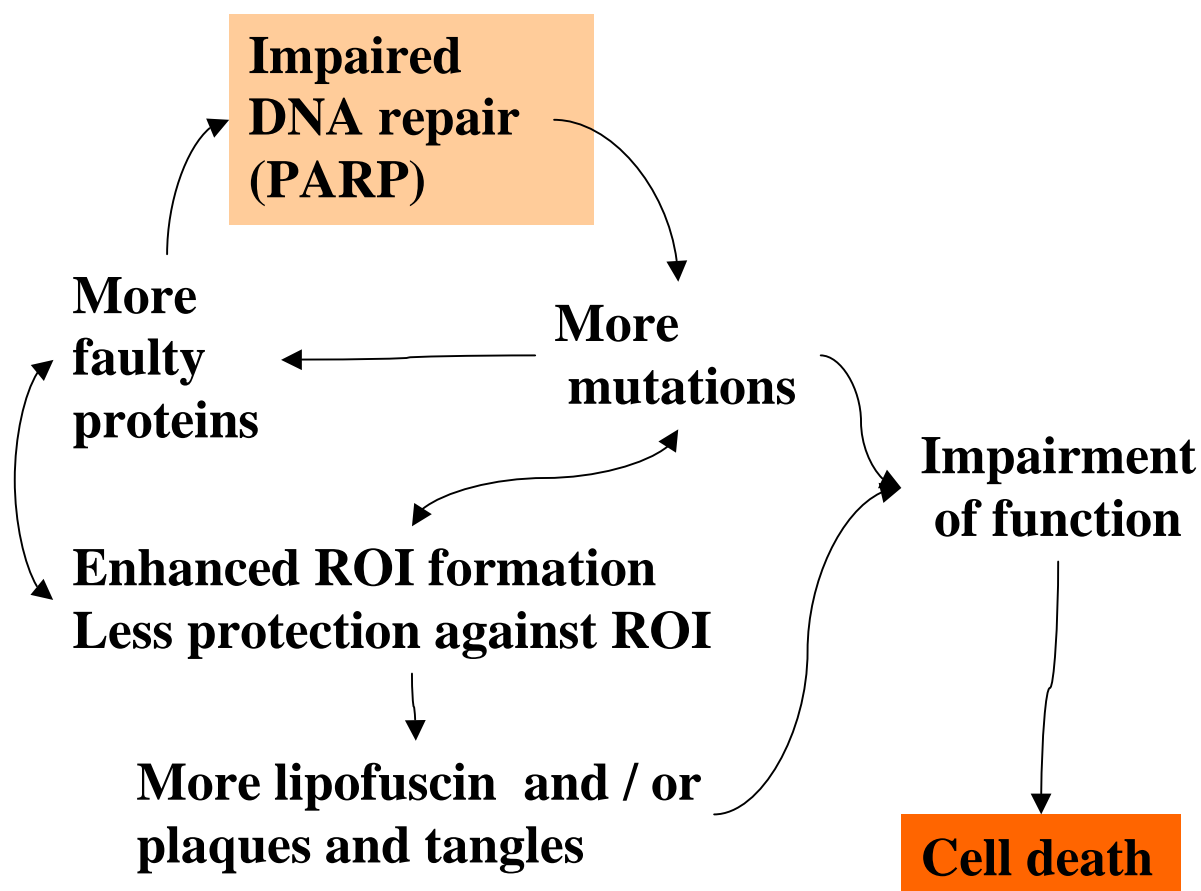


Fig. 6. Simplified hypothetical scenario of the ageing process in non-dividing, post-mitotic cells. ROI formed by the cell's normal metabolic activity cause damage to proteins and DNA, and the latter, if not accurately repaired, may represent pre-mutagenic lesions. In mitochondrial DNA, which replicates also in postmitotic cells, this may lead to mutation. In the nuclear genome, accumulated unrepaired DNA damage may lead to transcriptional errors across the damaged site altogether. Mutations occurring in open reading frames of genes can cause synthesis of faulty proteins. Faulty proteins themselves involved e.g. in DNA synthesis or DNA repair would then allow the accelerated formation of further mutations. Faulty proteins involved in the mitochondrial respiratory chain will cause the enhanced formation of ROI. Other proteins, if impaired, lose their function to protect against these ROI. An enhanced occurrence of ROI will then again cause an increased amount of impaired proteins, which in turn can cause mutations. In addition to these cycles insoluble deposits, such as lipofuscin, amyloid plaques and tangles, can begin to form. These deposits then can cause functional impairment at all levels of cellular metabolism, which may as well accelerate the cycles described above, until finally the overall impairment of cellular functions leads to cell death.

Proliferative cells on the other hand, can further be sub-divided into differentiated cells, stem cells and germ cells.

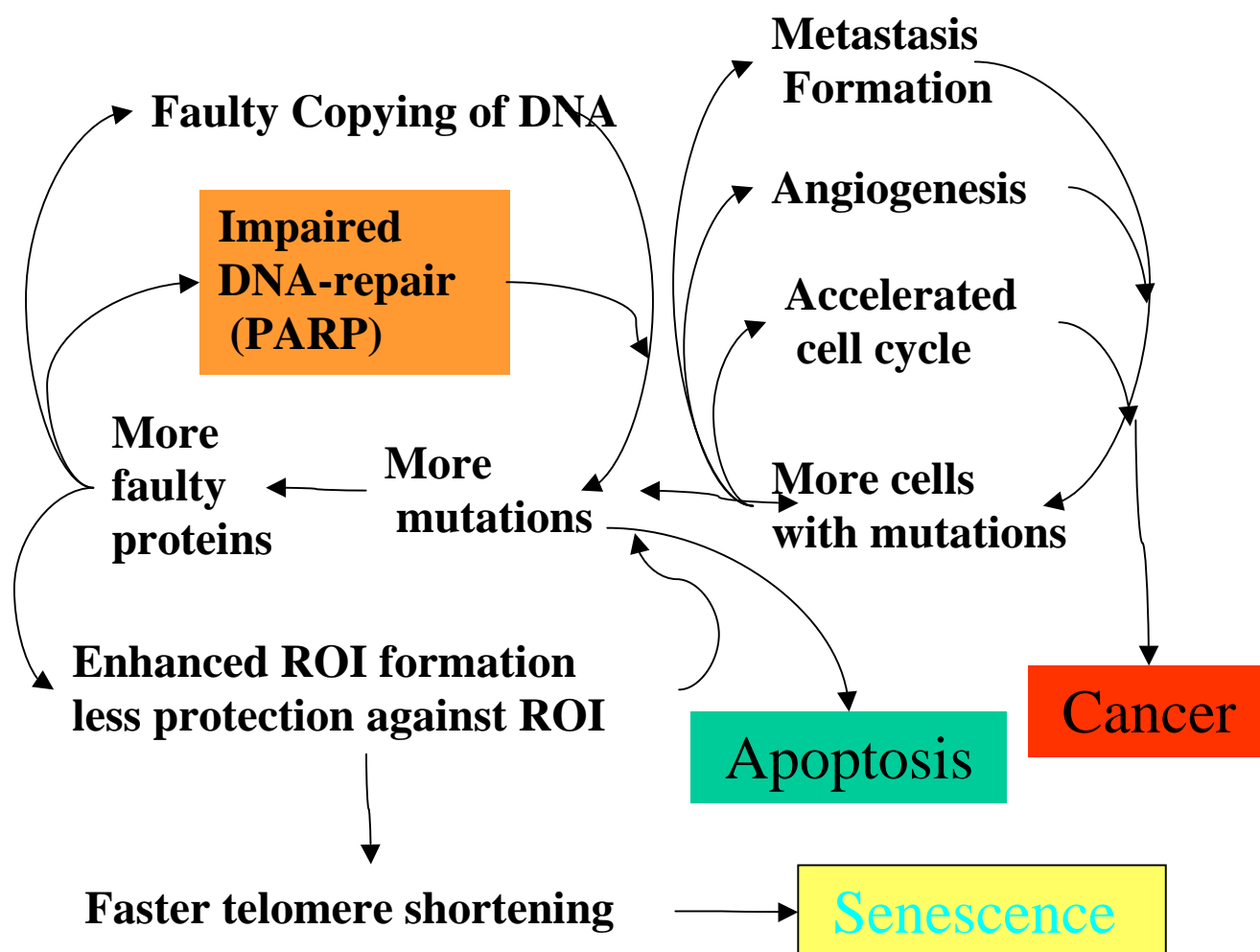


Fig. 7. Simplified hypothetical scenario of the ageing process in dividing cells. Initially, there are few errors at any stage of the cell function. The first inevitable errors then cause the subsequent degeneration of all systems that are vital for the cell. Reactive oxygen intermediates (ROI) cause the first mutations. Mutations occurring in open reading frames of genes can cause faulty proteins to be synthesised. Faulty proteins involved e.g. in DNA synthesis or DNA repair would then allow the accelerated formation of further mutations. Faulty proteins involved in the mitochondrial respiratory chain will cause the enhanced formation of ROI. Other proteins, if impaired, lose their function to protect against these ROI. More frequent occurrence of ROI would, in turn, lead to increased amounts of non-functional or dysfunctional proteins and accelerated telomere shortening which then can cause

earlier senescence. If the integrity and stability of the cellular genome decays beyond a certain limit, the cell will have to undergo apoptosis. Another kind of degeneration can involve the cell-cycle control of the cell. A possible consequence of faster cell division may be an increased risk of mutational error accumulation and therefore an increased risk of malignant transformation, with cells acquiring more and more features of the malignant phenotype such as angiogenesis or metastatic growth. In conclusion, cellular senescence, apoptosis and cancer can all be viewed as consequences of degeneration arising during, or being facilitated by, the ageing process. Interestingly stem cell compartments seem to be better protected against such degeneration.

In dividing cells different mechanisms of deterioration can be envisaged (Fig. 7). Dividing cells are at all times at risk to lose cell cycle control and to enter the multi-step pathway of carcinogenesis. Cellular senescence and apoptosis are presumably mechanisms protecting against cancer formation, but at the same time have to be viewed as mechanisms of degeneration.

Germ cells must be particularly well protected against accumulating errors. It might well be the case that entirely different mechanisms are active to protect them from deteriorating, which are not represented in Fig. 7.

Over the last decade, data have accumulated suggesting a scenario of how DNA repair, and PARP-1 in particular, may be involved in the control of such cascades of error accumulation and thus are emerging as longevity-assurance factors (Grube et al., 1992; Bürkle et al., 1994; Muiras et al., 1998, Meyer et al., 2000; Beneke et al., 2000; Bürkle, 2001 b,c,d).

I. 7. Current methods to detect and quantify poly(ADP-ribose)

Over the past three decades, a wide variety of analytical procedures have been developed to detect and quantify p(ADPr) formed in living cells or in subcellular systems, respectively (de Murcia & Shall 2000).

Jacobson and colleagues (1984) have established a method that detects and quantifies p(ADPr) formed endogenously in living cells and comprises biochemical extraction, purification and enzymatic degradation of p(ADPr) to yield unique monomeric nucleosides, followed by fluorescent derivatisation and finally reversed-phase HPLC separation and fluorescence-based detection and quantification of polymer-derived nucleosides. This method still serves as the “gold standard” in the field, but is expensive, laborious and requires very large cell numbers, which is prohibitive for analyses of large numbers of samples.

Another, much simpler, method to estimate endogenous polymer formation in living cells has been developed by Bürkle and colleagues (1993; Schlicker et al., 1999; Seker et al., 2000). In this method cells are grown on or adhered to cover slips and then treated with damaging agents. Thereafter cells are fixed with TCA and washed with ethanol (Fig. 8). As a first antibody the anti-p(ADPr) monoclonal 10H is used. As a second antibody fluorescein isothiocyanate-labelled anti-mouse immunoglobulin is used. The readout is done under the microscope comparing cells subjected to various treatment conditions with controls. Quantification of the result is possible but very laborious. This assay would also be inappropriate for very large sample sizes.

An assay originally developed by Berger and colleagues (1979) measures p(ADPr) formation in permeabilised cells (Fig. 8). It is based on radioactively labelled NAD^+ , the ADP-ribosyl moiety of which is incorporated into the polymer and thus becomes acid-insoluble. The readout is done by liquid scintillation counting of TCA insoluble material. Addition of a short double-stranded oligonucleotide to the reaction buffer leads to dose-dependent stimulation of polymer formation above background (Grube et al., 1991).

Many interesting results have already been obtained using this “Berger” assay *e.g.* a correlation between longevity in mammals and maximal p(ADPr) formation (Grube & Bürkle 1992) and higher maximal poly(ADP-ribosyl)ation capacity in centenarian-derived cells than in controls (Muiras et al, 1998). However, major drawbacks are the use of radioactivity, including expensive radioactive tracers, the relatively large cell numbers needed, and problems with complete removal of any unincorporated NAD⁺ from TCA precipitates. In this dissertation a new, non-isotopic and simple method for the assessment of poly(ADP-ribosyl)ation capacity is presented (Fig. 8).

Berger 1979	Jacobson 1983	Bürkle 1993	Pfeiffer 1999
<ul style="list-style-type: none"> -Preparation of cells -Permeabilisation of cells -Polymer formation with radioactively labeled NAD⁺/ oligo -Cell ghosts dotted on Whatman filter washing with TCA / Ethanol -Liquid scintillation counting 	<ul style="list-style-type: none"> -Intact cells -Precipitated with TCA -Release of polymer from proteins by EDTA / alkali treatment -Denaturing of proteins with 6 M Guanidine DHBB column purification of polymer -Digestion of polymer into phosphoribosyl -AMP by Snake venom phosphodiesterase -Alkaline Phosphatase treatment to ribosyl-Adenosine -Chloro-acetaldehyde treatment to create etheno-derivatives (fluorescent) -HPLC separation with fluorescent readout. 	<ul style="list-style-type: none"> -Cells grown on cover slips -Fixation with TCA -EtOH washing -1st Ab: anti-poly-(ADP-ribose) -2ndAb: FITC conjugated anti mouse -Readout under microscope -Quantification possible 	<ul style="list-style-type: none"> -Preparation of cells -Permeabilisation of cells -Polymer formation with unlabeled NAD⁺/ oligo -Cells dotted on membrane -TCA precipitated -Ethanol washed -Antibody incubation -Chemiluminescence readout.
Assay measures :	Assay measures:	Assay measures:	Assay measures:
Maximal polymer formation in permeabilised cells	Endogenous polymer formation in living cells	Endogenous polymer formation in living cells	Maximal polymer formation in permeabilised cells

Fig. 8. Scheme summarising available assays to detect and quantify poly(ADP-ribose)

I. 8. Current methods to measure DNA damage and repair

The two currently most popular methods to measure DNA damage and repair at highest levels of sensitivity are the ‘comet’ assay (reported detection limit 0.05 Gy; Singh, 2000) and the

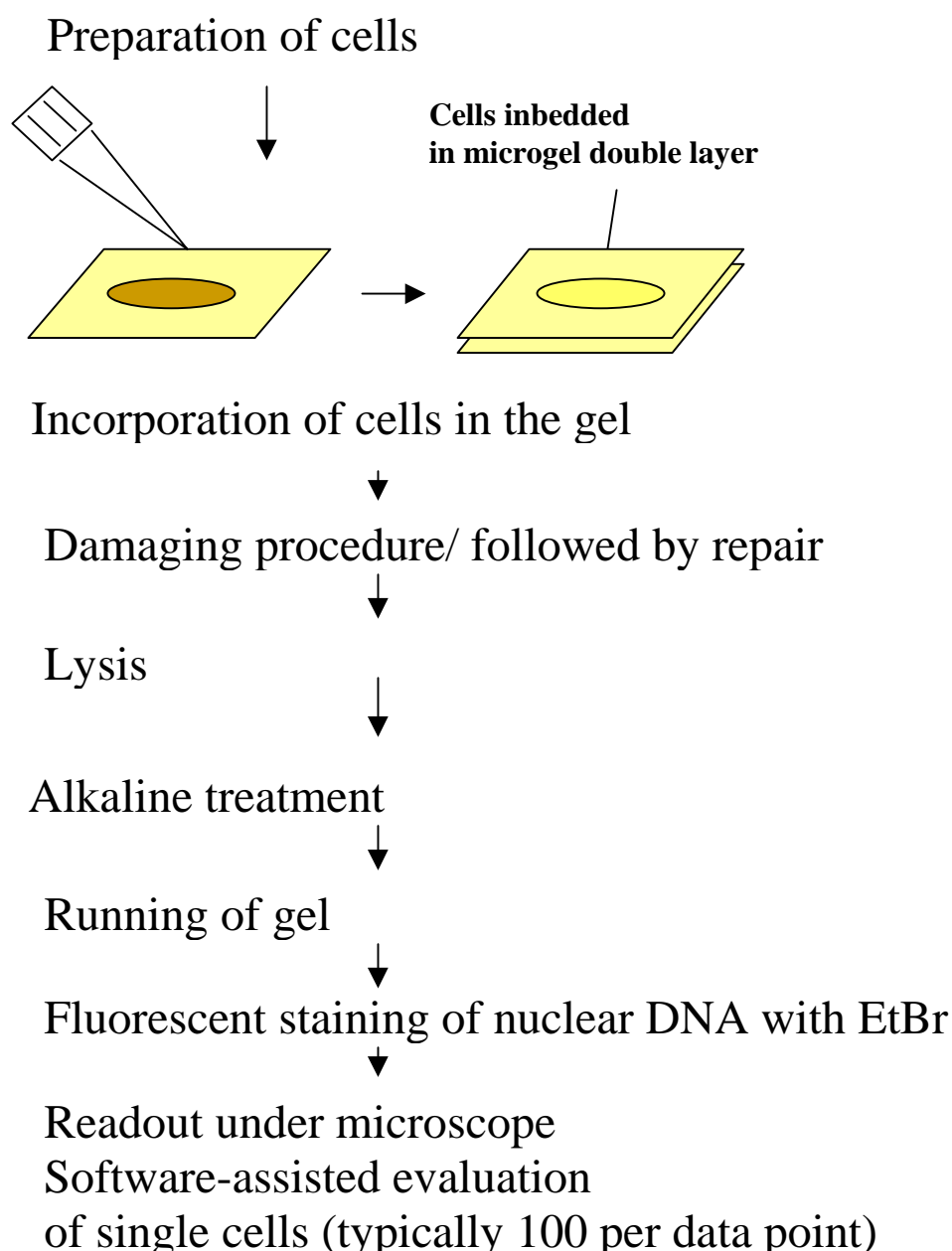


Fig. 9. Schematic overview describing the steps of the experimental procedure of the comet assay. Cells resuspended in a buffer are added to a first layer of a gel. Then a second layer of gel is cast enclosing the single cells. Cells are exposed to DNA-damaging agents in the gel, which may be followed by repair period. Then cells are lysed in situ and treated with alkali. After electrophoresis, the gel has to be stained and washed. The readout of the stained DNA of the single cells has to be done under a microscope. The tail moment of comets can be evaluated by quantitative digital imaging.

fluorescence-detected DNA unwinding assay (FADU) (reported detection limit 0.1 Gy; Singh, 2000).

The mechanisms underlying these two assays differ from each other. The principle of the comet assay is based on different migration velocities of DNA fragments of different size in agarose gels. The more single-strand breaks have been introduced into the DNA, the smaller the single-stranded fragments of the DNA will be and the faster these fragments will migrate in an electric field applied to the gel. Therefore, whole cells are embedded in an agarose gel, lysed and treated *in situ* with alkali to render the DNA single-stranded prior to running the gel. (N.B. A neutral version of this assay can be used to quantify double strand breaks). In an appropriate electrical field, the genomic DNA migrates out of the nucleus into the agarose and is then stained with the intercalating fluorescent dye ethidium bromide, allowing visualisation of the DNA. Viewed microscopically the combination of the DNA that has stayed within the confines of the nucleus and the “tail” of DNA that has migrated makes individual cells look like comets. Quantitative microscopic evaluation is done by measuring the length and intensity of the comet in relation to the signal of the non-migrating nuclear DNA in comparison with standards (Fig. 9).

The principle of the FADU assay is based on the fact that double-stranded DNA exposed to defined, moderate alkaline conditions unwinds at a constant rate, starting at its natural ends as well as at internal single or double-strand breaks. As a result, there will be more extensive unwinding of DNA carrying strand breaks (Fig.10.). This effect can be quantified using chemical probes that intercalate preferentially or exclusively into double-stranded DNA and become fluorescent by being intercalated. Thus the fluorescent signals obtained are an (inverse) increase of different levels of DNA breakage present in the cells at the time of lysis.

The manually performed FADU assay as originally published by Birnboim and Jevcak (1981) is very tedious and difficult to standardise, hence hardly used any more.

The comet assay has been improved in recent years (Sing, 2000), *e.g.* by establishing evaluation software to assist the readout procedure. Nevertheless, it is also still very tedious, as gels have to be prepared and processed manually in a multi-step procedure (Fig. 9).

In this dissertation, an automated version of the FADU assay is presented. Using an appropriately designed laboratory robot, all the critical and tedious pipetting steps have been automated and are performed under strict temperature control and protection from light. Furthermore the readout has been radically simplified by using a 96-well fluorescence reader instead of single cuvettes (Fig. 11).

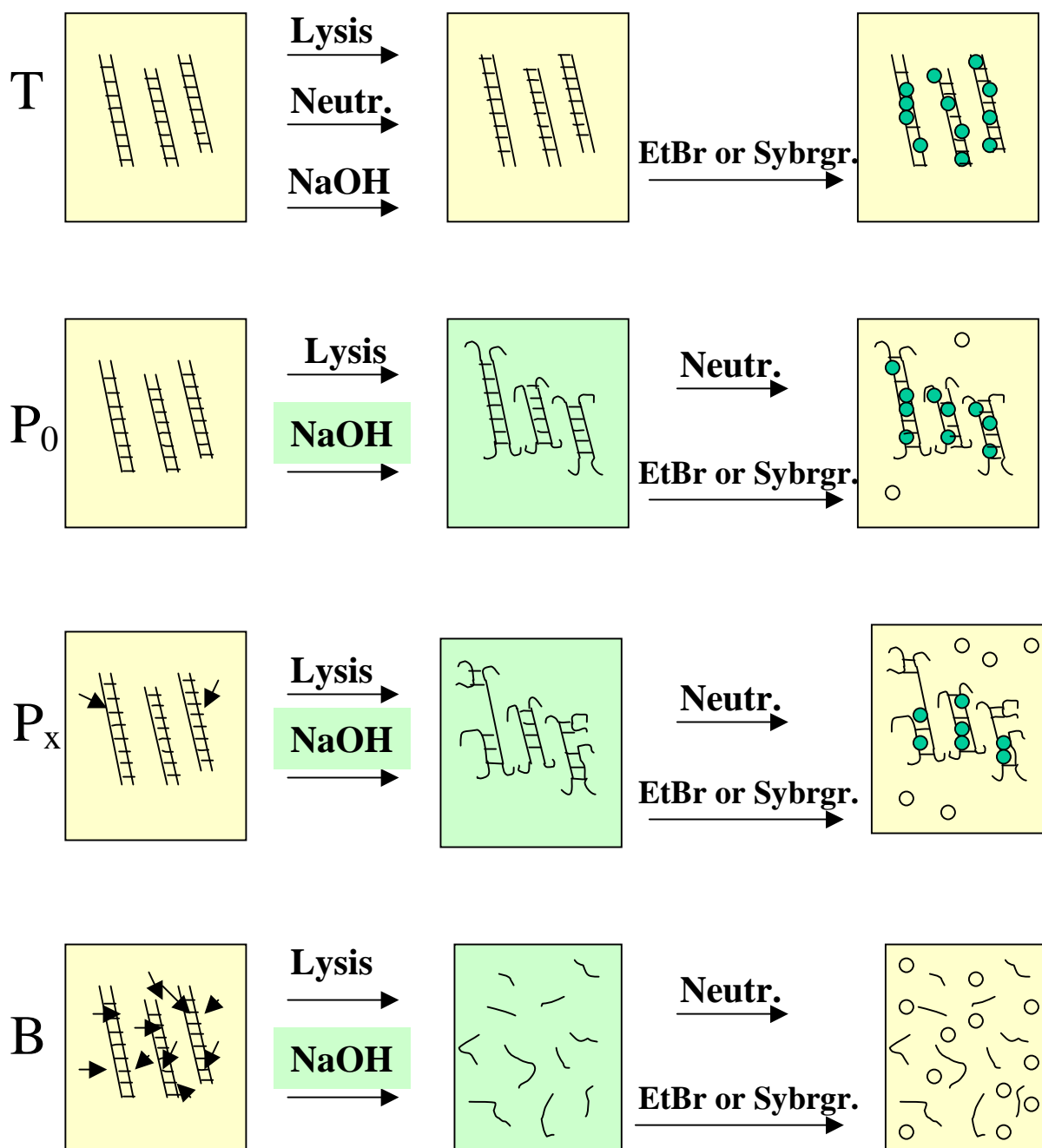


Fig. 10. Principle of the fluorescence-detected alkaline DNA unwinding. Double stranded DNA is represented as double lines. DNA strand breaks are indicated by arrows. Following cell lysis by detergents and disruption of chromatin by high concentrations of urea, cellular DNA is exposed to alkali under rigorously controlled conditions with regard to pH, temperature and time. Alkali exposure is achieved via diffusion from a separate layer placed on top of the lysate, rather than by

direct mixing, which would introduce artificial strand breaks. To the “T-samples, neutralisation buffer is added before the alkali so that the solution never reaches a pH necessary for unwinding. Alkaline unwinding in the P and B values starts only at the ends of chromosomes or at single and double-strand breaks. The more damage has been introduced into the DNA the less double-stranded DNA will remain after the unwinding phase. To stop unwinding, neutralisation buffer is added to the P and B values. For detection ethidium bromide or Sybr green (open circles) is added to all samples. These dyes intercalate preferentially into double stranded DNA inducing their fluorescence (filled green circles). The more double stranded DNA has remained, the more intense the fluorescent signal will be.

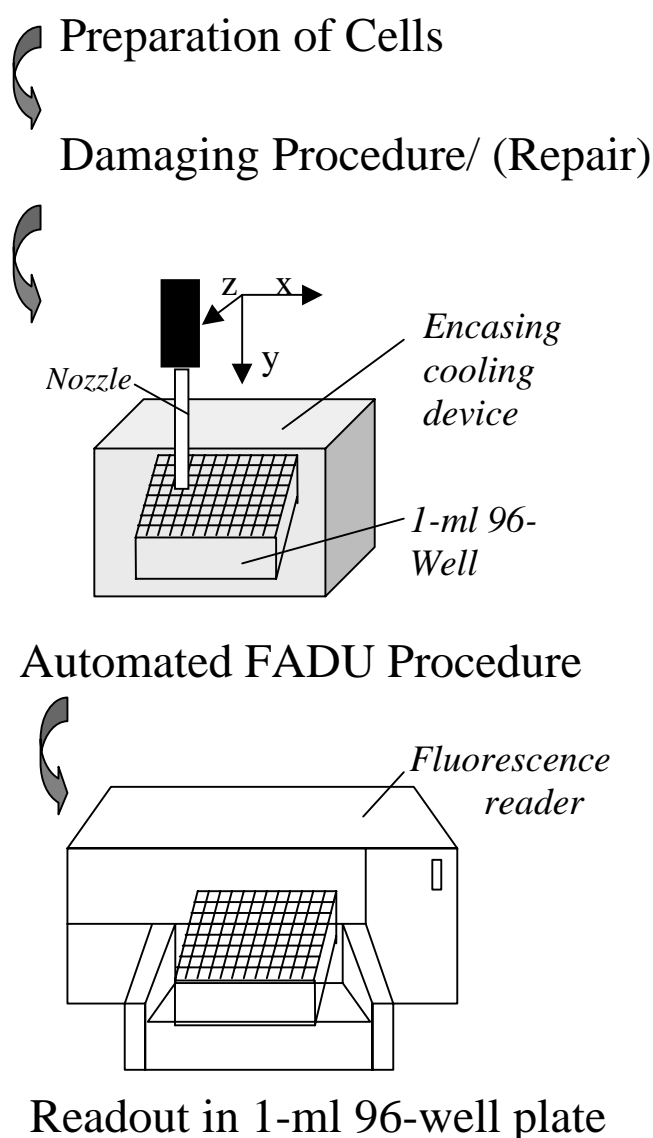


Fig. 11. Schematic overview depicting the experimental procedure of the automated FADU assay. Only the preparation of cells and the damaging procedure/ (repair) have to be done manually. The assay itself is fully automated. The readout is done in a 1-ml 96-well plate.

As a result, the throughput, accuracy, reliability and operator convenience have been increased dramatically, thus enabling large-scale analyses that should be of interest to a wide range of laboratories engaged in basic biomedical research or applied toxicology as well as to pharmaceutical companies.

I. 9. Aim of the project

Quantitative assessment of exogenous DNA damage and also of DNA repair activities is of utmost importance not only for a broad range of basic scientific research fields but also for routine tasks, such as medical monitoring of patients or probands to assess individual genotoxic exposures and the body's response to them, as well as toxicological screening in the chemical and pharmaceutical industry or monitoring of environmental pollution.

However, there is also a growing demand to assess endogenous DNA damage and its repair. The rapidly increasing fraction of elderly people in almost all countries worldwide and the increased awareness of the additional morbidity and the forthcoming strain to health-care systems resulting from this demographic change highlight the importance of understanding the process of ageing at the molecular level. The latter is indispensable for the development of urgently needed novel, rational modalities of prophylaxis or therapy of ageing-associated pathologies. Over the past few years much evidence has already accumulated supporting a critical role for endogenous macromolecular damage (including DNA damage) as a driving force of the ageing process at the cellular level, leading to decreased stress resistance and increased vulnerability of cells and tissues (Bürkle, 2001 d). In particular, the past and current work of Dr Bürkle's group has been focussed on the impact of poly(ADP-ribosyl)ation and BER on the ageing process in mammals.

Grube & Bürkle (1992) have described a correlation between maximal lifespan of mammalian species and poly(ADP-ribosyl)ation capacity. Muiras et al (1998) have observed higher specific poly(ADP-ribosyl)ation capacity in lymphoblastoid cell lines derived centenarians compared to controls. Meyer et al (2000) have found that PARP-1 overexpression protects against DNA damage-induced sister-chromatid exchange. Beneke et al (2000) have discovered that purified PARP-1 of humans possesses twice as much automodification activity as purified PARP-1 of rats. These observations are very much in line with a report by

Kapahi et al. (1999) describing that fibroblasts from long-lived mammalian species are more resistant to a variety of stresses, including genotoxic stress.

The above-mentioned results as well as data from other laboratories lead to the present working hypotheses:

- Somatic cells from long-lived organisms should be genetically more stable, mediated at least in part by their higher poly(ADP-ribosyl)ation capacity.
- Long lived organisms should possess more proficient DNA repair systems (already shown for NER, but as yet unknown for BER).

To be able to address these questions experimentally, two technologies had first to be further developed. One of them is a non-radioactive immuno-dot-blot assay to assess poly(ADP-ribosyl)ation capacity (Pfeiffer et al, 1999). This assay should help establish whether PARP-1 can serve as a marker of human ageing. Furthermore, with the recent discovery of PARP homologues, it was extremely interesting to check if this type of assay is specific for PARP-1 or will also reflect PARP-2 activity.

The second technology that needed substantial improvement beyond the present state of the art was the FADU assay. This assay was first described in 1981 but was seldom used, even though it had been reported to possess very high sensitivity. The reason for this is that it is very difficult to perform and even very skilled and highly motivated lab workers were unable to run it in a reproducible manner (Dr Alexander Bürkle, personal communication). Another significant disadvantage was the large number of cells required.

The aim of the present PhD work was to set up automation of the FADU assay, along with miniaturisation by downscaling of the procedure to the 96-well format. It was desired that apart from preparation of cells and the DNA-damaging treatment, all pipetting steps (*i.e.* sequential additions of defined buffers to the primary cell lysates) should be carried out by a laboratory robot, with a single 96-well plate serving as the basic matrix for the whole procedure, including readout of the samples in an appropriate fluorescence reader. Predictably such an assay format should be much more convenient to operate than other current methods including the comet assay.

Given the laboratory's specific research interests in biogerontological research, one of the first applications (out of a vast range of possible applications) then was to determine BER capacity as a function of lifespan in mammals (see above).

From the above considerations, it is also clear that successful establishment of improved methods for the assessment of DNA damage and repair should also facilitate research on, or routine monitoring of, exogenous genotoxic exposures.

II. Materials and Methods

II. 1 Appliances

⁶⁰Co-gamma-irradiation device (Gammacell 1000 Elite, Nordion Inc, Canada);

1-ml 96-Well plates. These were made from commercial 2-ml 96-well plates (Masterblock, Greiner Labortechnik) by cutting them down to a height of 2.0 cm thus accommodating 1 ml in each well. The plate is levelled thus enabling sealing of all wells simultaneously with Parafilm. The plates can be re-used after washing with 1M NaOH and then with DMSO and ethanol. A volume of 1 ml per well and a height of 2.0 cm of the plate are the largest dimensions suitable for use in the 96-well fluorescence reader.

To control temperature in the 1-ml 96-well plate a self-made **cooling device** (Fig. 12) was assembled from commercially available polypropylene plates, in which water tubing encases the 1-ml 96-well plate. For each of the 96 well positions, a hole was drilled from the top between the tubing thus enabling the diluter of the robot to access all 96 wells, while the plate is inserted in the cooling device. An ethanol-water mixture (1:3) of desired temperature is circulated through the tubing using a **Lauda 2000** water bath.

Pipetting robot, Miniprep I (Fig. 12) (Tecan, Crailsheim, Germany) with one arm, carrying a single stainless steel nozzle

Fluorescence reader (Spectrafluor Plus, Tecan, Crailsheim, Germany);

Multi-channel pipette (Sealpette 1200, 12 channels, Jencons, UK)

Heraeus Biofuge 3 (Heraeus, Germany)

Thermomixer 5436 (Eppendorf, Hamburg, Germany)

24-well dot-blot manifold, custom-made with well diameter of 1.2 cm (Steinbrenner Laborsysteme GmbH, Eberbach, Germany).

LAS-1000 chemoluminescence detection system (Fuji; Raytest, Straubenhardt, Germany)
in conjunction with „Aida“ software (Raytest)

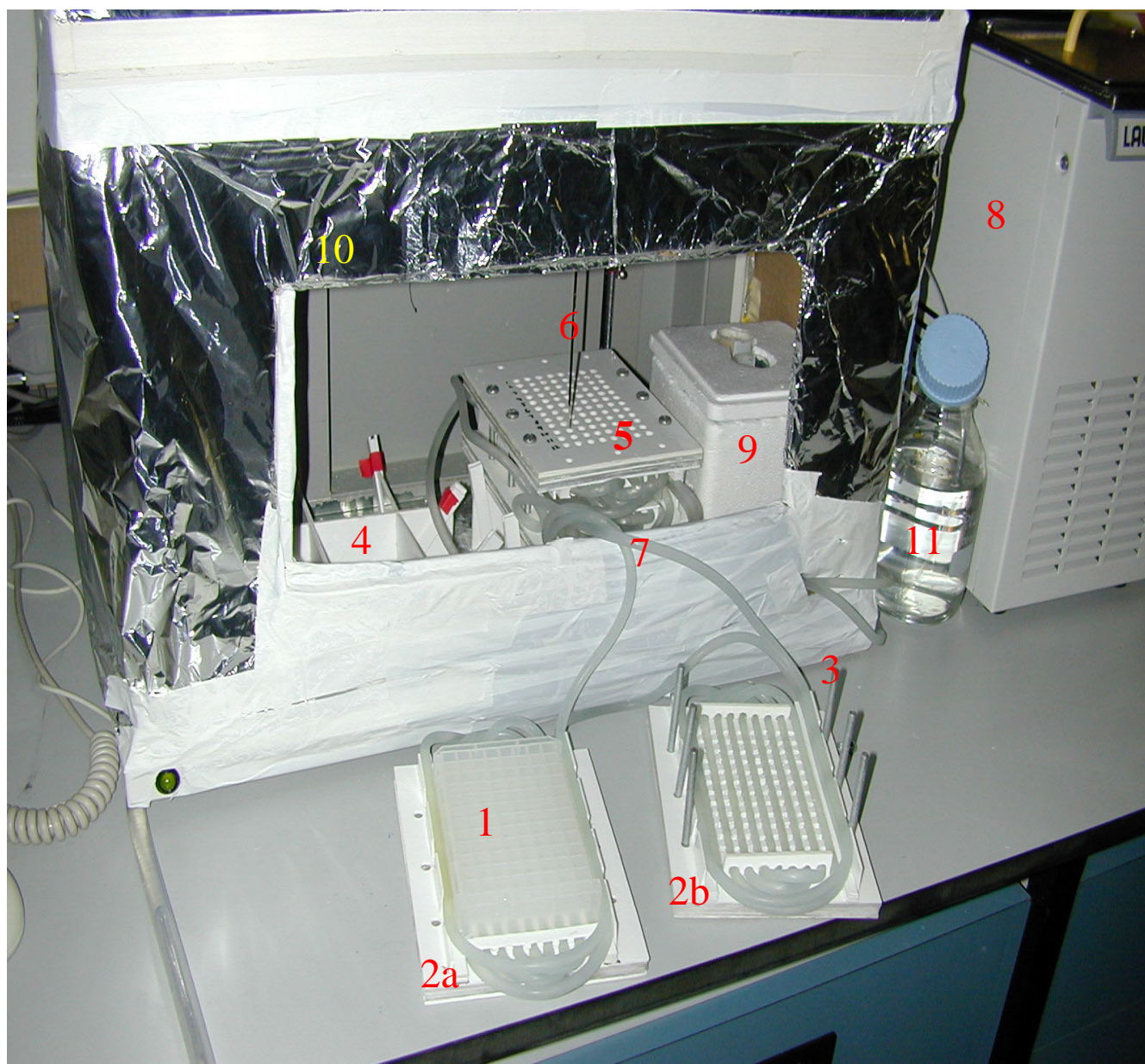


Fig. 12. Pipetting robot set up for the FADU assay. (1) Transparent custom-made 1-ml 96-well plate, which is inserted in (2a) the lower part of the self-made cooling device. (2b) The upper part of the cooling device, with 96 holes for the nozzle to pass through, has been turned over and during operation will be placed on top of the lower part (2a) and fixed with six bolts (3) and nuts. Encasing the 1-ml 96-well plate, the cooling device is then placed on its stand (4) i.e. in a position within the working area of the robot defined at a precision of 0.2 mm. A sister plate (5) is already in its stand. The nozzle (6) precisely finds its target with regard to X, Y, Z coordinates. The water tubing (7) is connected to the water bath (8) for temperature control. Ice cold buffers are stored in a little ice box (9) accessible to the nozzle from the top. For protection against light the working area is enclosed by cardboard wrapped in aluminium foil (10). It can be closed with a lid (not visible). Washing liquid for the nozzle (11).

II. 2. Chemicals

„ECL plus“ kit	Amersham-Pharmacia (Germany).
β-Mercaptoethanol	Sigma (Germany)
NAD ⁺ (grade V)	Sigma (Germany)
Digitonine	Sigma (Germany)
3-Aminobenzamide	Sigma (Germany)
TCA	Roth (Germany)
Sodium pyrophosphate	BDH (UK)
NaCl	Merck (Germany)
Tris	Merck (Germany).
Magnesium sulfate	Merck (Germany).
DMSO	BDH (UK)
Ethanol	BDH (UK)
Ethidium bromide	Merck (Germany)
EDTA	Merck (Germany)
Glucose	Merck (Germany)
Urea	BDH (UK)
Sybr green	Raytek (Germany)
Skimmed Milk Powder	Fluka (Germany)
Sodium hydroxide	BDH (UK)
Penicillin	Sigma (Germany)
Percoll	Amersham Pharmacia (Germany)
Trypsin (0.5 μg / ml)	BRL (Germany)
Tween 20	Gerbu (Germany)

II. 3. Oligonucleotides

The PARP-1 activator deoxyoligonucleotide (GGAATTCC) was dissolved in 15 mM NaCl at 385 μg/ml. The 3'- and 5'-termini of the oligonucleotide were unphosphorylated.

II. 4. Antibodies

Mouse monoclonal antibody recognising p(ADPr) was purified from culture supernatant of 10H hybridoma cells (kind gift of M. Miwa and T. Sugimura, Tokyo, Japan) by using a protein-A column chromatography kit (Sigma). This was done by Mr Marcus Müller in the laboratory.

Peroxidase-conjugated anti-mouse secondary antibody (Dianova, Hamburg, Germany)

II. 5. Membranes

--Gene Screen membrane (NEN, Brussels, Belgium)

--Nitrocellulose membrane (Biometra, Germany)

III. 6. Buffers and solutions

--Permeabilisation buffer: 10 mM Tris-HCl pH 7.8; 1 mM EDTA; 4 mM MgCl₂; 30 mM 2-mercaptoethanol, with or without 0.015% (w/v) digitonine supplementation as indicated

-- PBS-MT: PBS pH 7.4; 5 % semi skimmed milk powder; 0.05 % Tween 20

--PBS-T: PBS pH 7.4; 0.05 % Tween 20

--Percoll solution: 63 % Percoll [Amersham Pharmacia]; 0.15 M NaCl in H₂O

--EDTA solution: 10 mM ethylenediaminetetraacetate, pH 8.4

--Suspension buffer: 0.25M *meso*-inositol, 10 mM sodium phosphate pH 7.4, 1 mM MgCl₂

--Lysis buffer: 9 M urea; 10 mM NaOH; 2.5 mM cyclohexyl-diaminetetraacetate; 0.1% sodium dodecylsulfate

--Alkali solution: 0.425 parts lysis buffer in 0.2 M NaOH

--Neutralisation buffer: 1 M glucose, 14 mM β -mercaptoethanol

--Sybr green solution: 13.3 mM NaOH; Sybr green (1:25.000)

II. 7. Cell culture medium

RPMI 1640 medium (Sigma) supplemented with 100 U/ml penicillin, 100 μ g/ml streptomycin, 2 mM glutamine, and 10% heat-inactivated foetal calf serum (Sigma). Cultures were incubated at 37°C/5% CO₂.

DMEM medium (Gibco) supplemented with 100 U/ml penicillin, 100 μ g/ml streptomycin, 2 mM glutamine, and 10% heat-inactivated foetal calf serum (Sigma). Cultures were incubated at 37°C/5% CO₂.

II. 8. Cell lines

IARC 273, Epstein-Barr virus immortalised human B-lymphoblastoid cell line (kind gift of Dr M Pawlita, DKFZ, Heidelberg, Germany)

3T3 Embryo fibroblast cell line from PARP-1^{-/-} mice

3T3 Embryo fibroblasts cell line from PARP-1^{+/+} mice (wild-type control)

(kind gift of Dr Gilbert de Murcia, ESBS, Université Louis Pasteur, Strasbourg, France)

II. 9. Animals and human blood donors

The rat strain used was Fischer 133.

Blood was obtained from nine months old rats (4 females and 2 males) after killing. This was performed by highly trained and authorised animal care staff, in compliance with the relevant national laws and regulations.

Human blood donors were healthy volunteers from diverse ethnic groups. All human blood donors were adult but not older than 41 years, which corresponds to one third of the maximum life span of humans of 123 years.

III. Methods

III. 1. Poly(ADP-ribose) immuno-dot-blot assay

Cell permeabilisation and p(ADPr) formation assay. IARC 273 cells were washed in PBS, resuspended in ice-cold permeabilisation buffer supplemented with 0.015% (w/v) digitonine at a density of 3×10^6 cells/100 μ l and left on ice for 1 min. Then 4 ml of ice-cold permeabilisation buffer was added. Cells were centrifuged at 1000 x g, 0°C for 10 min and resuspended in ice-cold permeabilisation buffer at a density of 5×10^5 cells per 53 μ l. To samples of 5×10^5 cells on ice was added 13 μ l of oligonucleotide solution and 34 μ l of 3x reaction buffer (100 mM Tris-HCl, pH 7.8, 1 mM NAD⁺, 120 mM MgCl₂), respectively, resulting in a total volume of 100 μ l per reaction. The reaction was carried out for the times indicated at 30°C on a shaker and stopped by adding 400 μ l of 6.25 mM 3-aminobenzamide in PBS on ice.

Detection procedure. Volumes of the reaction mixture as indicated were vacuum aspirated onto a Gene Screen membrane by using a 24-well dot-blot manifold. Before the membrane dried completely, 400 μ l of 10% TCA (w/v), 2% sodium pyrophosphate (w/v) was filled into the manifold, and 800 μ l of 70% ethanol was carefully layered on top of this. The two layers were vacuum aspirated. Then the membrane was rinsed in PBS, blocked in PBS-MT and incubated with the first antibody (10H; 2.5 μ g/ml in PBS-MT) overnight at 4°C, with constant agitation. Thereafter, the membrane was washed with PBS-T and incubated with peroxidase-conjugated anti-mouse secondary antibody (1:10,000 in PBS-MT) for 1 h at room temperature. The blot was washed with PBS prior to chemoluminescence detection by using the „ECL plus“ kit.

Standardisation of p(ADPr) quantity. ADP-ribose polymer was purified from TCA precipitates of some of the samples by dihydroxyboronate chromatography, followed by enzymatic digestion to nucleosides, fluorescent derivatisation and quantification of polymer-specific nucleoside derivatives during reversed-phase HPLC separation, as described (Jacobson et al., 1984).

III. 2. Automated fluorescence detected alkaline DNA unwinding assay

Separation of mononuclear lymphocytes

Six ml of whole blood from human donors was collected with a syringe, with 60 μ l EDTA solution present as an anti-coagulant. Then the blood was diluted 1:2 with PBS, layered on top of 15 ml Percoll solution and centrifuged at 1500 g using a Heareaus Biofuge. Mononuclear cells were recovered, washed once with PBS, centrifuged at 1000 g and resuspended in suspension buffer at a concentration of 10^6 cells per ml. For measuring repair, the cells were resuspended in DMEM without FCS and other supplements at a concentration of 10^6 cells per 150 μ l.

DNA damaging procedure

150 μ l cell aliquots in Eppendorf tubes were cooled down to 0°C and irradiated on ice for different time periods with a ^{60}Co -gamma source at a dose rate of 3.6 Gy per min in air.

DNA repair

To assess repair, cells damaged at 2.7 Gy were incubated at 37°C for various time periods on a Thermomixer, with a shaking frequency of 50 rpm to allow strand break repair to proceed. To stop repair 850 μ l ice cold suspension buffer was added on ice.

Lysis and DNA unwinding procedure

70 μ l of all cell samples, which had been treated differently, was added to the 1-ml 96-well plate, respectively, and kept at 0°C in the dark working space of the robot. Then automated addition to all samples of 70 μ l of lysis buffer at a rate of 150 μ l / s was triggered. Subsequently the alkali solution was added on top of the cell lysate in such a way that a second layer was forming, thus avoiding any mixing with the lysate. To do this the robot positioned the nozzle precisely 1.5 mm above the level of the lysate and added the alkali solution at a very low rate of 10 μ l / s. This was done in such a way as to allow exactly 12 min time for lysis (*i.e.* the preceding step) for each well. Then 15 min were allowed for the diffusion of the alkali into the lysate at 0°C. Then the temperature was shifted to 30°C for 90 min. Prior to the addition of 140 μ l of neutralisation buffer at a rate of 200 μ l / s the temperature was shifted to 22°C. For T-samples, as an internal standard representing cells with 100 % double stranded DNA, 140 μ l of neutralisation buffer was added prior to the

alkaline solution. In some experiments B-samples were included as an internal standard representing cells with 0 % double stranded DNA as a result of extensive of the lysate prior to addition of alkali, i.e. by passing the lysate 20 times through a 0.5 mm cannula. In course of the work it was noted that there was an excellent correlation between T and B values, and since the B values were quite low in the case of Sybr green, B samples were omitted from the final FADU version.

Readout

To perform the readout, 470 μ l Sybr green solution was added with an automated multi channel pipette (Sealpette). The wells of the 1-ml 96-well plate were then sealed with Parafilm and the plate turned upside down 10 times. To reach an equilibrium the solution was allowed to rest precisely 10 min before scanning by a 96-well plate fluorescence reader at Em 492 nm and Ex 520 nm.

IV. Results

IV. 1. Setting up a new immuno-dot-blot procedure to assess cellular poly(ADP-ribosylation) capacity.

Assessment of the maximal cellular p(ADPr) formation (termed “poly[ADP-ribosyl]ation capacity”) has proven very interesting in a wide range of studies performed by many laboratories over the last three decades (Althaus & Richter 1987; de Murcia & Shall 2000, Bürkle 2001a,b). Unfortunately the available standard technique required use of expensive radioactively labeled tracers (^3H - or ^{32}P -NAD⁺) and, in addition, was fraught with problems arising from insufficient removal of unincorporated tracer from acid-insoluble product to be quantified (*i.e.* p[ADPr]), thus requiring multiple parallel determinations in view of the frequent outliers (*cf.* Muiras et al., 1998).

Assuming that an appropriate immuno-dot-blot procedure that would rely on the excellent binding specificity of monoclonal anti-p(ADPr) antibody 10H (Kawammitsu et al, 1984; Bürkle et al, 1993) could be viable alternative, a set of preliminary experiments was performed to test a range of commercially available blotting membranes for their potential usefulness (not shown). Membranes were loaded with permeabilised cells that had been incubated under conditions allowing maximal accumulation of p(ADPr) [see below]. One of the most promising candidates turned out to be the nylon membrane ‘Gene Screen’. To determine more accurately its binding capacity, permeabilised IARC 273 lymphoblastoid cells were incubated with unlabeled NAD⁺ as substrate and “activator” oligonucleotide (GGAATTCC) for 6 min at 30°C, allowing maximal p(ADPr) accumulation to occur (Grube et al, 1991). The reaction was stopped by adding the competitive ADP-ribosylation inhibitor 3-aminobenzamide and cooling on ice. The cell ghosts were then directly dot-blotted onto the membrane, followed by TCA precipitation *in situ*, washing with ethanol and immunodetection of p(ADPr) by using monoclonal antibody 10H in conjunction with a peroxidase-based chemoluminescence detection system.

As a first step the reaction kinetics of the polymer formation under the conditions of the dot blot procedure was examined (Fig. 13.). It was found that there is an almost linear increase during the first four minutes followed by a plateau and a slight decrease at around 8 minutes. Six minutes were chosen as a standard reaction time for all subsequent experiments.

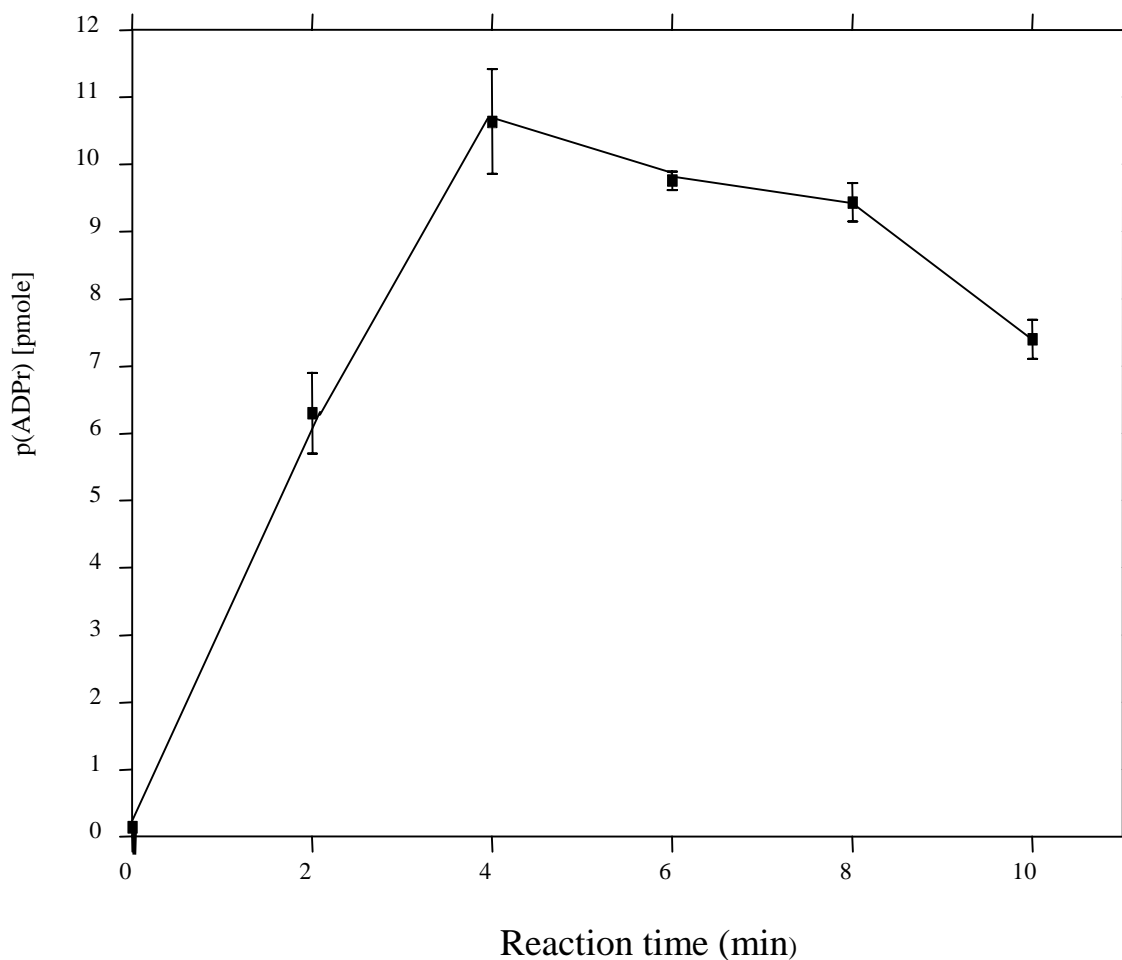


Fig. 13. p(ADPr) formed in IARC 273 cells as a function of reaction time. 60,000 permeabilised IARC 273 cells were incubated in reaction buffer at 30°C for varying time periods as indicated. Note that there is an almost linear increase in p(ADPr) formed during the first 4 minutes, followed by a plateau and a slight decrease at around 8 minutes.

In Fig. 14 is shown the intensity of chemoluminescence signals obtained as a function of cell number. The curve is linear up to 120,000 cells per blotting area (113 mm²), while above this

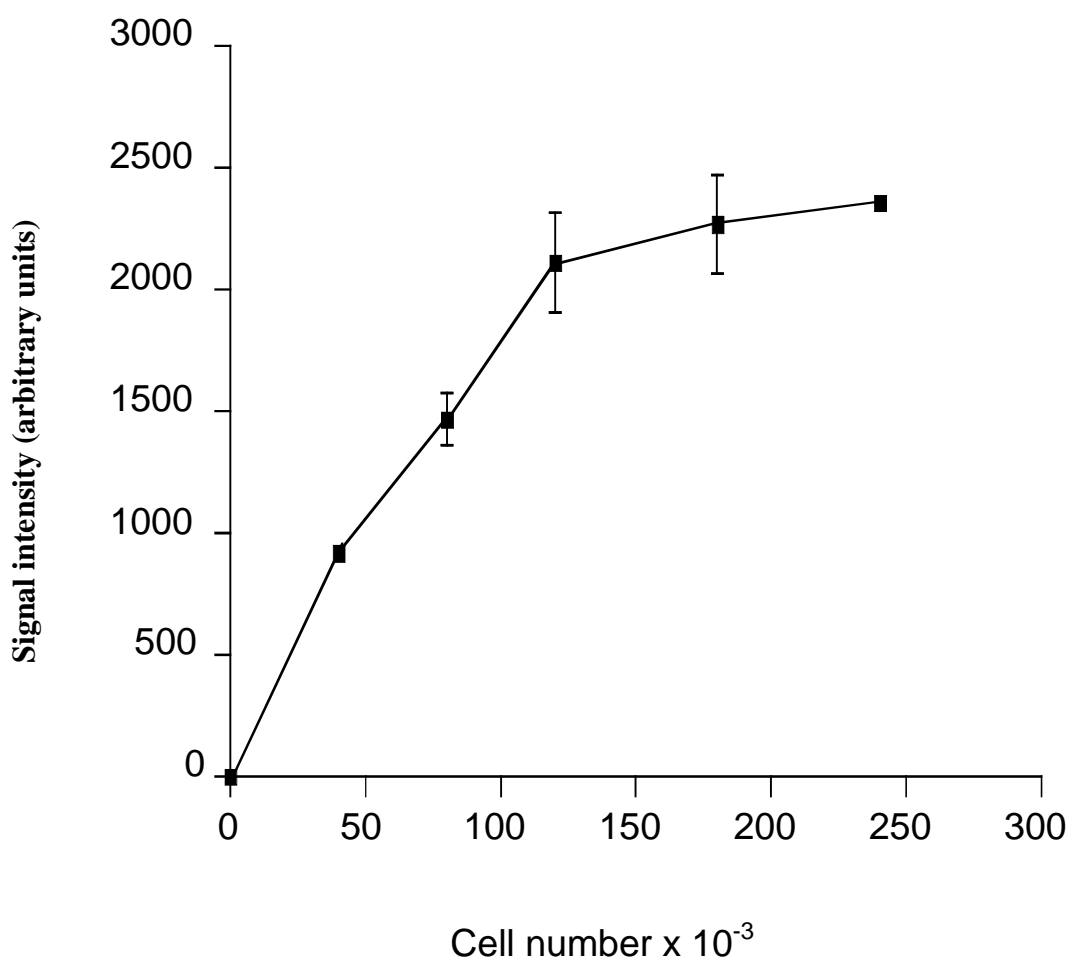


Fig. 14. Binding capacity of Gene Screen nylon membrane for permeabilised IARC 273 cells. 40,000 to 240,000 permeabilised cells that had been incubated with NAD^+ and activator oligonucleotide for 6 min at 30°C were loaded on the membrane, followed by TCA precipitation in situ and immunodetection of p(ADPr) as described in Materials and Methods. Quantification of chemoluminescence signals was performed by using a Fuji LAS1000 detection system. Mean values ± 1 SD (if larger than symbol size) are represented. Note that chemoluminescent signals are linear up to 120,000 cells loaded per blotting area (113 mm²).

cell number saturation of the membrane is apparent. No significant differences between an uncharged (Gene Screen) and a positively charged (Hybond N+; Amersham-Pharmacia) nylon membrane were found (data not shown). Nitrocellulose proved unsuitable, as it does not withstand exposure to 10% TCA.

To determine the filter binding characteristics of varying amounts of p(ADPr) present in a constant number of cells, mixtures of permeabilised IARC 273 cells that had been incubated in reaction buffer for 6 min at 30°C, to allow extensive p(ADPr) formation, with cells that had not been incubated were loaded on Gene Screen membranes. A total of 60,000 cells were applied, which included 0, 25, 50, 75 and 100 % of buffer-incubated cells, respectively (Fig. 15). As is apparent from Fig. 15, increasing amounts of p(ADPr) resulted in a linear increase in signal intensity. It should be noted that blotting areas of > 100 mm² proved very useful, since permeabilised cells tend to form clusters, and this clustering effect is averaged by using relatively large blotting areas.

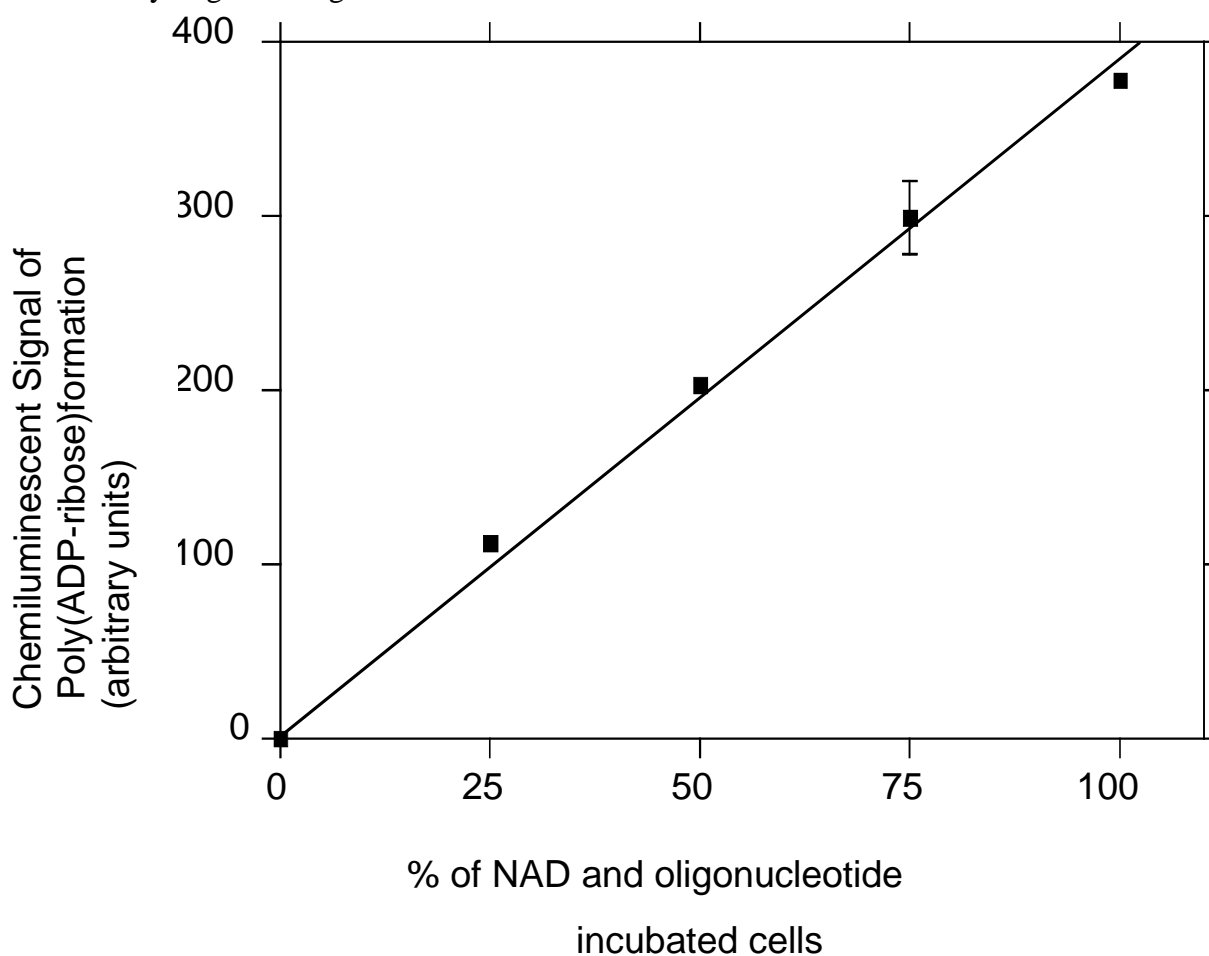


Fig. 15. Nylon membrane binding of increasing amounts of p(ADPr) with a constant number of dot-blotted cells. Mixtures of permeabilised IARC 273 cells that had been incubated with NAD⁺ and activator oligonucleotide for 6 min at 30°C with cells that had not been incubated were loaded on a Gene Screen membrane. In all cases, a total of 60,000 cells were applied. The mixing ratio is indicated as the percentage of NAD⁺/oligonucleotide-incubated cells present. Note that the p(ADPr) content per 60,000 cells incubated for 6 min at 30°C in reaction buffer was 8.1 pmole, while permeabilised control cells contained 20.9 fmole, as determined by HPLC-based quantification.

To determine the absolute amounts of p(ADPr) formed in permeabilised IARC 273 cells, quantification of p(ADPr) was done by Ms Christine Brabeck in the laboratory, using a standard method based on HPLC separation and fluorescent quantification of specific p(ADPr) breakdown products (Jacobson et al, 1984). In the experiment shown in Fig. 15, the p(ADPr) content per 60,000 cells incubated for 6 min at 30°C in reaction buffer was 8.1 pmole, while 60,000 permeabilised control cells contained only 20.9 fmole.

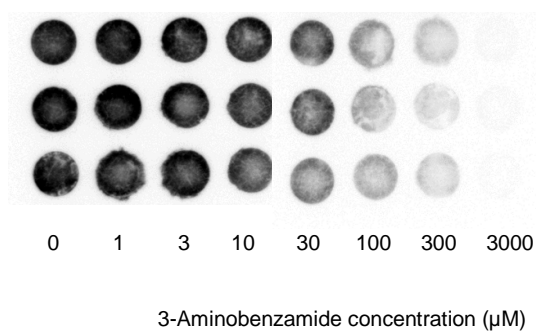
IV. 2. Evaluation of the new poly(ADP-ribose) immuno-dot-blot assay.

Next the applicability of this novel immuno-dot-blot technique was evaluated, using the paradigm of measuring PARP inhibitor potency. Since the abrogation of PARP activity has been shown to prevent tissue damage under a variety of pathophysiological conditions (de Murcia & Shall, 2000; Bürkle 2001b), the development of improved PARP inhibitors as novel drugs for the rescue of neurones, myocardial tissue, or pancreatic islet cells is of rapidly growing interest to basic researchers as well as to the pharmaceutical industry (Bürkle, 2001b). In the experiment shown in Fig. 16, permeabilised IARC 273 cells were incubated with reaction buffer in the presence of the prototype inhibitor 3-aminobenzamide as indicated. A clear-cut, dose-dependent inhibition of the formation of p(ADPr) was found. The IC_{50} detected by the present assay (39 μ M) compared very well with data from the literature (Banasik et al., 1992). These results show that, among other uses, present method is indeed suitable for the identification and characterisation of PARP-inhibitory substances.

With the recent discovery of PARP homologues, it was extremely interesting to check if this type of assay is specific for PARP-1 or will also reflect PARP-2 activity, *i.e.* the other DNA damage-activated member of the PARP family. While activation of PARP-2 by nicks in double stranded DNA has already been shown (Amé et al., 1999), it was not clear if the double-stranded blunt-ended activator oligonucleotide used in the new immuno-dot-blot assay would also lead to significant PARP-2 activation. To clarify this point, 3T3 fibroblast cell lines derived from PARP-1 knockout mice (PARP-1^{-/-}) were compared with wild-type mouse derived lines (PARP-1^{+/+}) (Fig. 17). While there was little p(ADPr) formation above the staining background in PARP-1^{+/+} cells (compare blue centre with blue left), there was a massive stimulation by the addition of activator oligonucleotide (blue right *vs.* blue centre), as expected (Grube et al., 1991). By contrast PARP-1^{-/-} cells produced very little p(ADPr) under

any condition, and there was only a marginal increase by the addition of oligonucleotide (red right vs. red centre). In conclusion, the vast majority of p(ADPr) formed in this assay in the presence of oligonucleotide reflects PARP-1 activity.

A



B

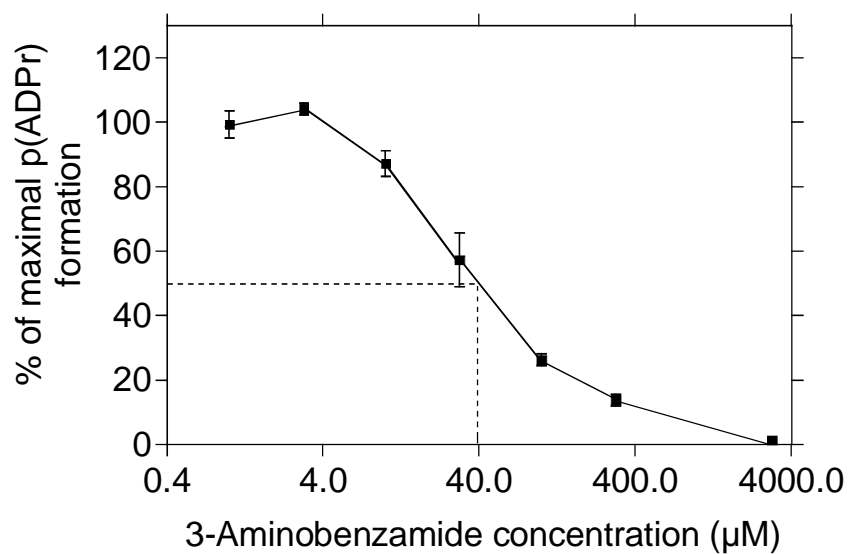


Fig. 16. Inhibitory effect of 3-aminobezamide on the formation of p(ADPr) in permeabilised IARC 273. Permeabilised cells were incubated with NAD^+ /oligonucleotide at 30°C for 6 min in the presence of 3-aminobenzamide as indicated. The IC_{50} detected by this assay is $39 \mu\text{M}$.

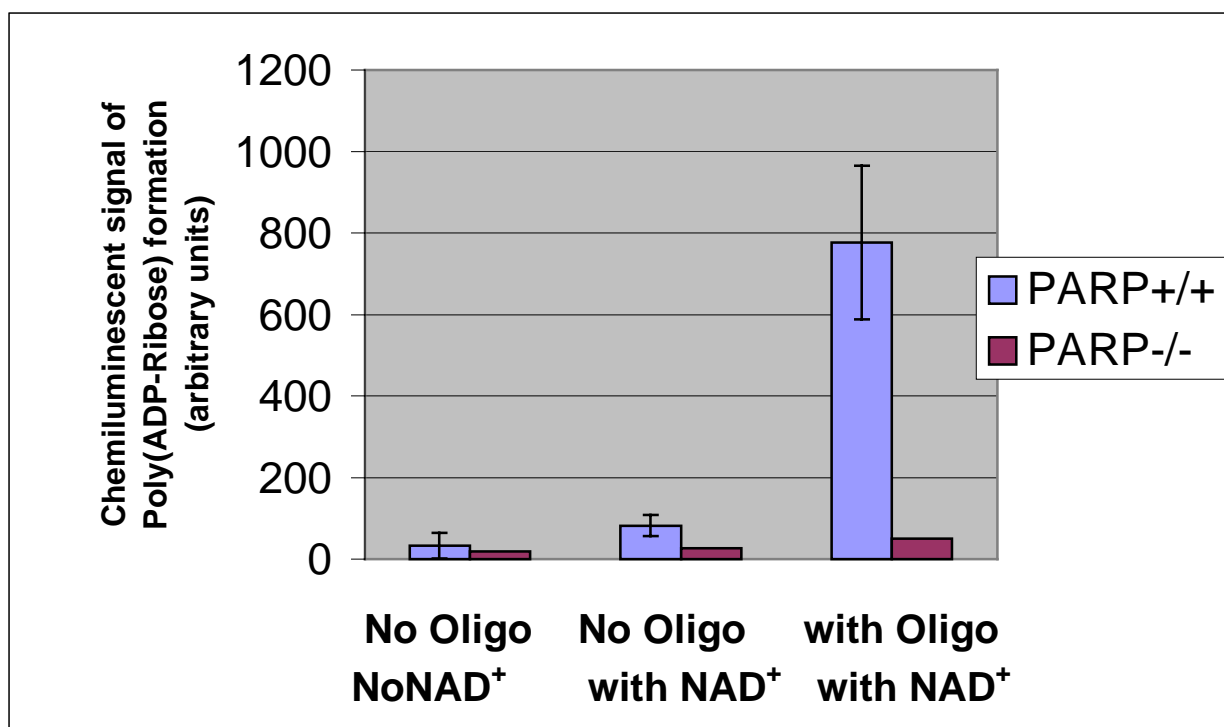


Fig. 17. Poly(ADP-ribose) formation in permeabilised mouse $PARP-1^{+/+}$ and $PARP-1^{-/-}$ cells. Mouse $PARP-1^{+/+}$ and mouse $PARP-1^{-/-}$ fibroblasts cell lines were processed according to the above described protocol under three different conditions, as indicated.

IV. 3. Setting up an automated version of the fluorescence-detected alkaline unwinding (FADU) assay to quantify DNA strand breaks and repair in live cells.

The automated and modified version of the FADU assay presented here enables measurement of DNA strand breaks and DNA repair in a very reliable and convenient manner. The basic strategic idea was to exploit the extremely high level of control of various parameters and reproducibility of pipetting small volumes afforded by laboratory robots, combined with the use of 96-well plates. Using robots, small volumes of liquids can be transferred at sub-millimetre precision within the three dimensions of the robot's workspace, with perfect control of both timing and rate (in $\mu\text{l/s}$) of uptake and delivery of, respectively. The latter is absolutely crucial for the step of forming a separate layer of the alkaline solution on top of the lysates without any mixing, which is the key step in the original FADU protocol. The possibility to encase the robot's workspace with light-proof material also adds enormously to

assay reliability, as the genomic DNA liberated from histones by the high urea concentrations present in the lysis buffer is very prone to artificial DNA breaks induced even by visible light (*cf.* Birnboim & Jevcak, 1981).

In a set of preliminary experiments the mechanics of robot-performed layer formation was investigated using addition of a visible dye as a marker to the alkaline solution and it was confirmed that layer formation without any mixing effect was reliably obtained in the 96-well format (not shown). Subsequently, the volumes of cell samples and solutions added in the course of the procedure described by Birnboim & Jevcak were scaled down to accommodate the reaction in 96-well plates (not shown). While this appeared to be possible to some extent, the reproducibility of the robot-operated assay was far from perfect at that stage.

To further optimise the procedure, the influence of 'lysis time' (*i.e.* the time between addition of lysis buffer and addition of the alkaline solution), which had been considered non-critical during the early phase of the work, on the performance of the assay was investigated. Standard assays were run with lysis times ranging from 5 to 90 min. The data showed that lysis times of up to 15 min do not affect the alkaline unwinding. Surprisingly, however, lysis times in excess of 15 min inhibited alkaline unwinding (Fig. 18). The reason for this is not known, but it may be speculated that prolonged incubation in lysis buffer favours cross DNA link formation. Therefore in the final automated FADU protocol, lysis time was set to be precisely 12 min for all 96 wells of a plate, thus precluding any artefact arising from variability of lysis time.

In the above, as in all subsequent experiments a single alkaline solution was used rather than two separate alkaline solutions "D" and "E" described in the original FADU protocol, with D to be layered on top of the lysate and then E on top of D. This represents a significant simplification of the procedure, which proved not to compromise assay performance (data not shown).

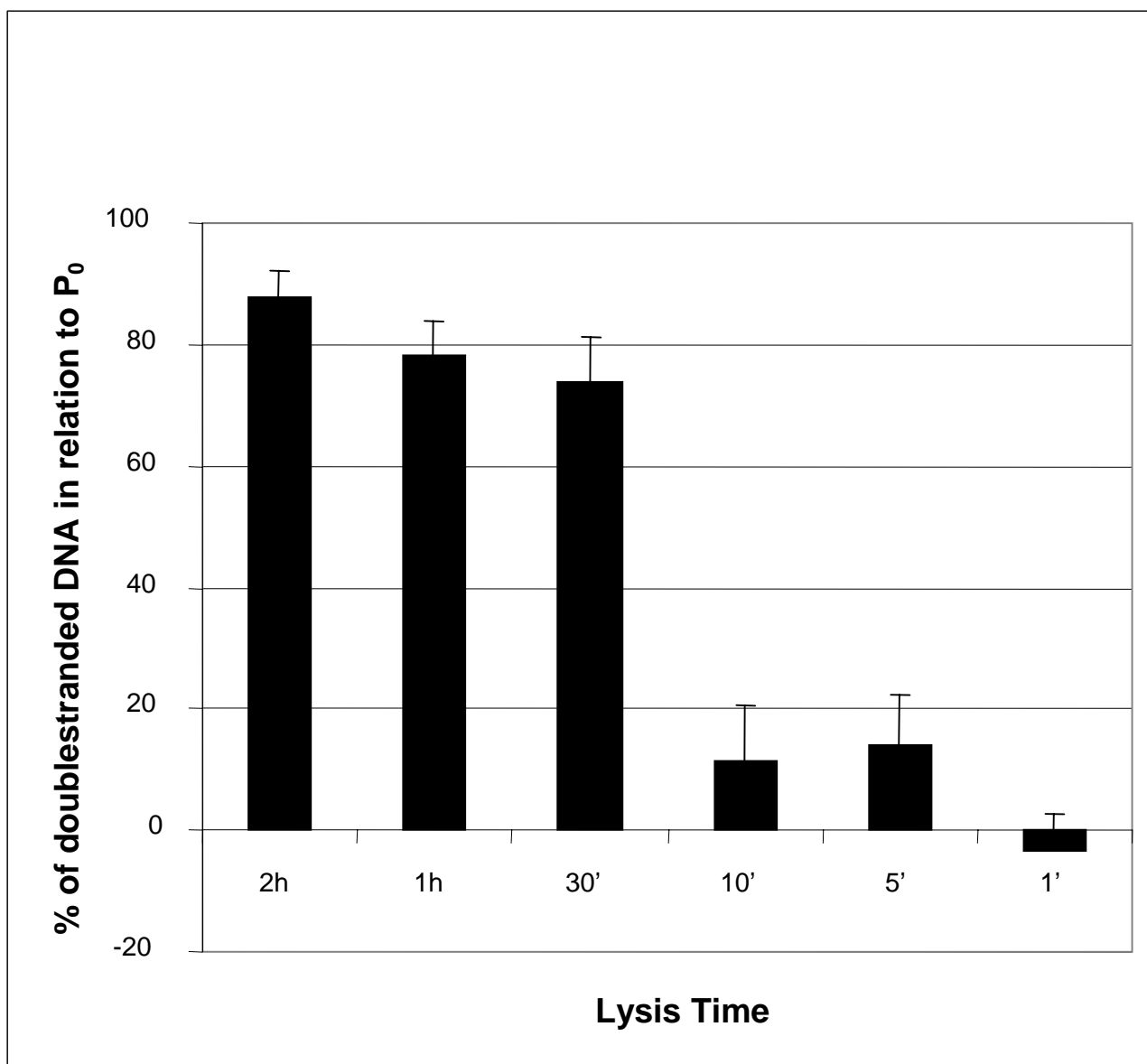


Fig. 18. Determination of optimal lysis time. IARC 273 cells (Epstein-Barr virus-immortalised human lymphoblastoid cell line) were resuspended in suspension buffer at 0°C at a density of 80,000 cells / 70 µl and dispensed as 70 µl-aliquots. For P₀ samples, cells were left undamaged. For P₄₀ samples, cells were exposed to 40 Gy γ-radiation on ice. Then lysis buffer was added at 0°C at a rate of 50 µl/s. On top of lysates, 70 µl of alkaline buffer was added at a rate of 10 µl / s. In the case of T-samples the latter was preceded by addition of 140 µl neutralisation buffer. Timing of the pipetting steps was set in such a way as to allow various time periods of lysis for different wells. Thereafter samples were incubated at 15°C for 90 min to allow DNA unwinding to occur. Then 140 µl of neutralisation buffer was added to B and P samples at a rate of 150 µl/s. For fluorescence-based readout, 150 µl of the samples was combined with 500 µl of ethidium bromide solution in single cuvettes, respectively. Fluorescence detection was performed in a standard fluorometer at Ex 480 nm and Em 520 nm. The data clearly indicate that lysis time is highly critical and only time periods of up to 15 min are suitable for the assay.

Another point of concern was the use of ethidium bromide for the fluorescence readout, as it is a mutagenic substance. It was therefore tested whether it is possible to substitute it with the less harmful compound Sybr green in the FADU protocol (Fig. 19). Not only proved this to be the case, but it turned out additionally that Sybr green created much less background than ethidium bromide, as revealed by the much lower B-sample fluorescence (*i.e.* in the absence of any double-stranded DNA by alkali-induced complete DNA denaturation in heavily sheared lysates). This means that the range for the measurements is considerably enlarged and thus assay sensitivity is increased.

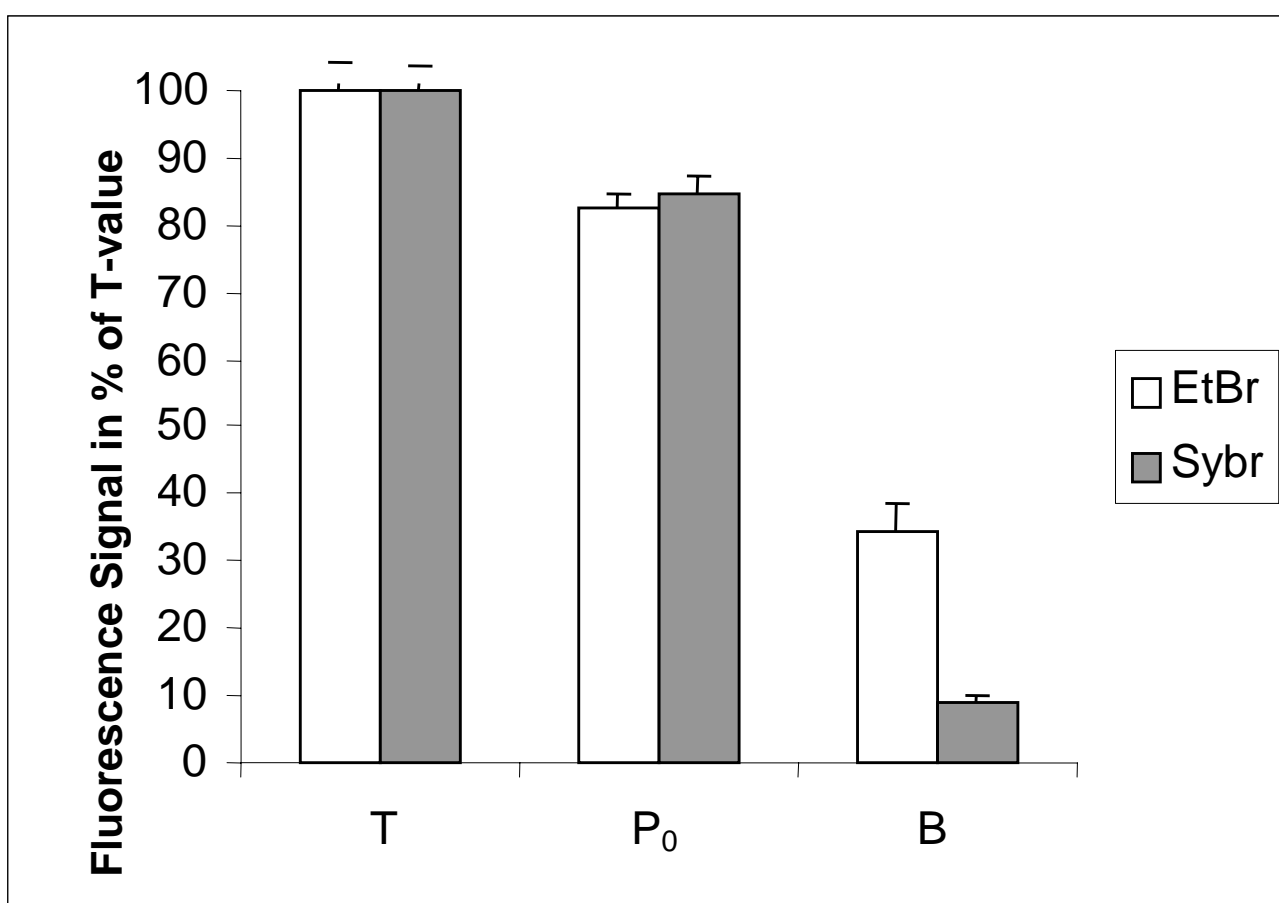


Fig. 19. Ethidium bromide in comparison to Sybr green. Mononuclear cells were isolated from human blood via Percoll gradient. For each experimental point 80,000 cells were suspended in 70 μ l suspension buffer at 0°C. For T and P₀ samples cells were not exposed to any damaging treatment. For B samples 70 μ l of lysis buffer was added to 70 μ l of cell suspension and the mixture was sheared by passing it 20 times through a 0.5-mm cannula. For P and T samples 70 μ l of cell suspension per well was filled into a standard 96-well plate. For B samples 140 μ l of the sheared lysate per well was filled into a standard 96 well plate. Then 70 μ l lysis buffer was added to P and T samples at 0°C. This step and all subsequent pipetting tasks were performed by the robot.

In case of T samples 140 μ l of neutralisation buffer was added. Then, 70 μ l unwinding buffer was added to B, P and T samples, respectively, without mixing, at precisely 12 min after addition of lysis buffer. Samples were then incubated at 15°C for 90 min to allow unwinding to occur. To stop the unwinding 140 μ l of neutralisation buffer was added to B and P samples, with mixing.

150 μ l of the reaction mixture was combined in plastic cuvettes with 500 μ l of either Sybr green solution or ethidium bromide solution at room temperature. Fluorescence detection was done at Ex 480 nm und Em 520 nm in a standard fluorometer (Hitachi 2000). The T/B ratio proved to be 2.5 for Ethidium bromide and 10 for Sybr green. Error bars represent ± 1 standard deviation of six-fold determinations.

To ensure that all wells were held at precisely the same temperature a self-made convection-operated cooling device consisting of polypropylene tubing (perfused with an ethanol / water mixture) and encasing the plate completely was used. Cooling only the bottom of the plate had turned out to be insufficient.

Furthermore, as is described in detail in Materials and Methods, an especially modified type of 96-well plate was used. Attempts to use standard commercial 96-well plates had failed (data not shown), as the volume of the initial cell suspension and the volumes of all subsequent buffers proved too small to be delivered with the high accuracy required.

In the final assay version, DNA strand breakage as inflicted by γ -radiation yielded a linear dose-response relationship in the dose range of 0 to 2.7 Gy (Fig. 20.). At higher doses there is a marked flattening of the curve, but nevertheless, damage can be quantified up to 20 Gy using appropriate calibration curves to linearise the data. Using shorter unwinding times even higher numbers of strand breaks can be quantified.

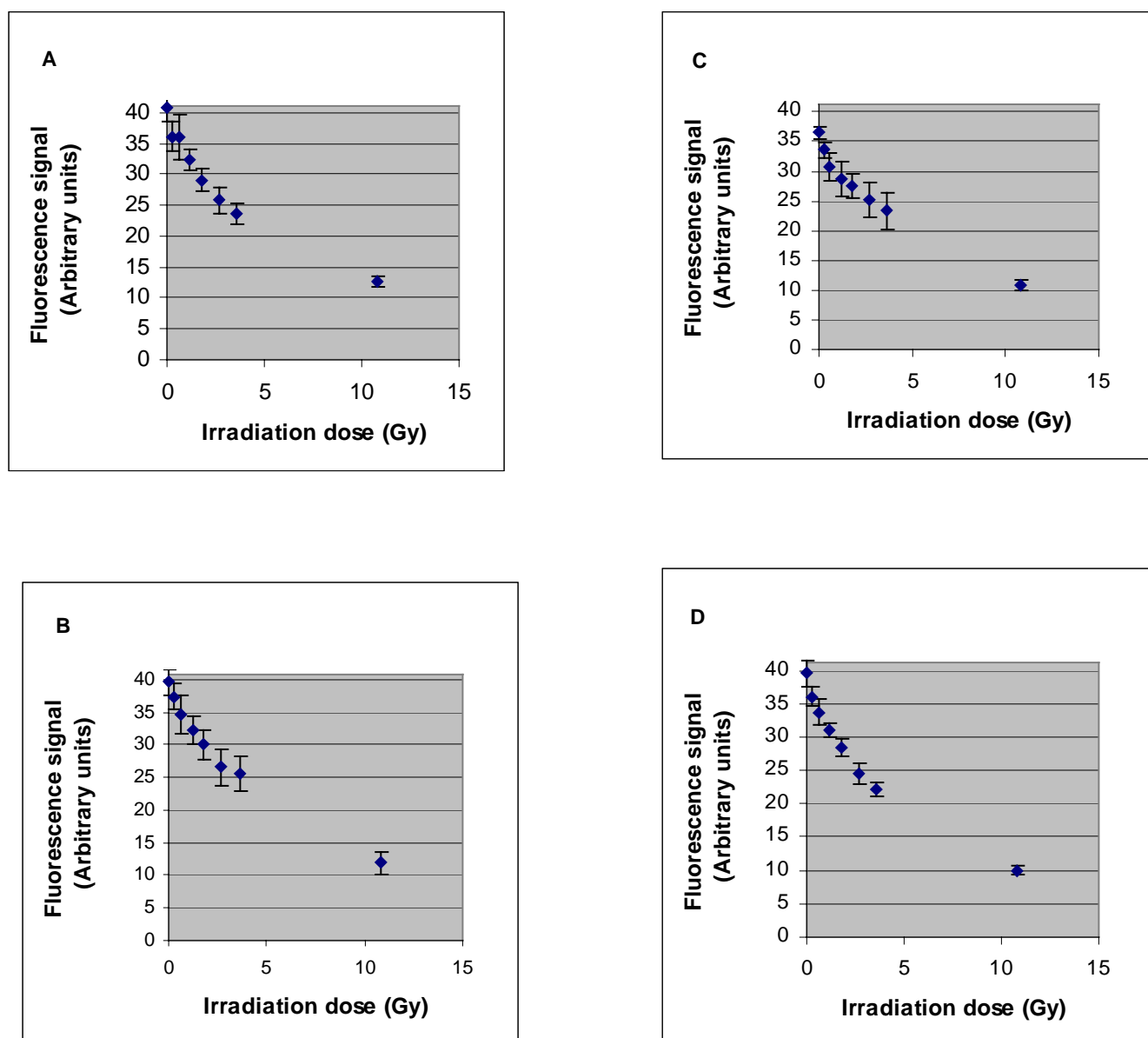


Fig. 20. Dose response curve of γ -radiation-induced DNA strand breaks in human mononuclear blood cells. Cells suspended in suspension buffer were irradiated on ice with varying doses of γ radiation as indicated. The cells were then treated as described in Materials and Methods. Each investigational point was carried out in twelve-fold determination. The T-value (i.e. non-irradiated cells that were not exposed to denaturing pH due to prior addition of neutralisation buffer) is represented in the figure as the upper end of the grey field. The assay was repeated on four consecutive days (A, B, C, D) with freshly obtained blood from the same human donor, respectively, demonstrating the excellent reproducibility of the assay. Between 0 and 2.7 Gy the assay yields a linear dose-response relationship. In all four independent experiments a damage level corresponding to 0.3 Gy could be detected with statistical significance ($p < 0.05$ by T-test in all four cases).

Using the automated finalised FADU method, also DNA strand break repair could be efficiently measured upon delivery of 2.7 Gy as damaging dose (Fig. 21.), thus exploiting the linear range of the dose-response curve (Fig. 20.). DNA repair was allowed to occur by incubating the irradiated cells in culture medium at 37°C for defined time periods.

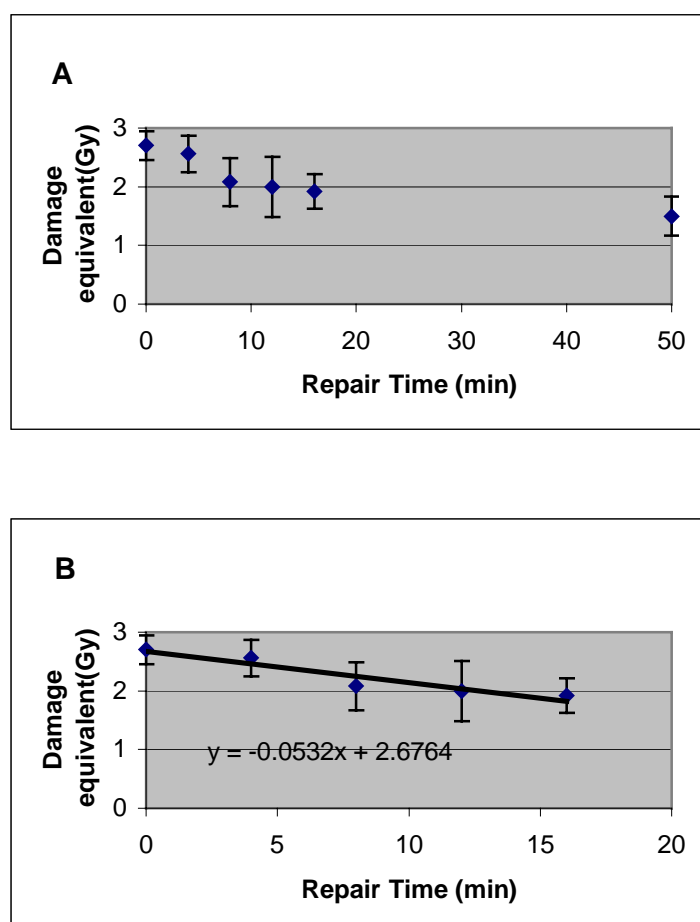


Fig. 21. Repair of DNA strand breaks after 2.7 Gy damage. Human mononuclear blood cells were given different time periods for repair at 37°C, as indicated, after an initial damage of 2.7 Gy γ radiation. It is evident from panel A that by 50 min, 50% of the initial damage was repaired and a plateau was reached. Panel B represents the slope of the initial phase of repair. $T_{1/2}$ (half-life time for repair, defined as the time needed to repair one half of the ‘repairable’ damage) was determined by linear regression analysis. In this experiment $T_{1/2}$ was 10.2 min, corresponding very well with data from the literature.

To assess the reproducibility of this kind of repair assay, 8 independent experiments using fresh blood from the same donor were performed within a time period of two weeks (Fig. 22). The data yielded an average strand break half-life of 10.9 min with a standard deviation of 1.41 min (13%). The average fraction of strand breaks repaired was 46 % with a standard deviation of 10% (Fig. 23). In view of the highly complex nature of the biological material used (*i.e.*, freshly obtained peripheral blood mononuclear cells) and the biological phenomenon studied (*i.e.*, the multi-step pathway of strand break repair), the above values are evidence for excellent assay reproducibility, which should encourage use of this assay in population studies in the context of ageing and cancer research.

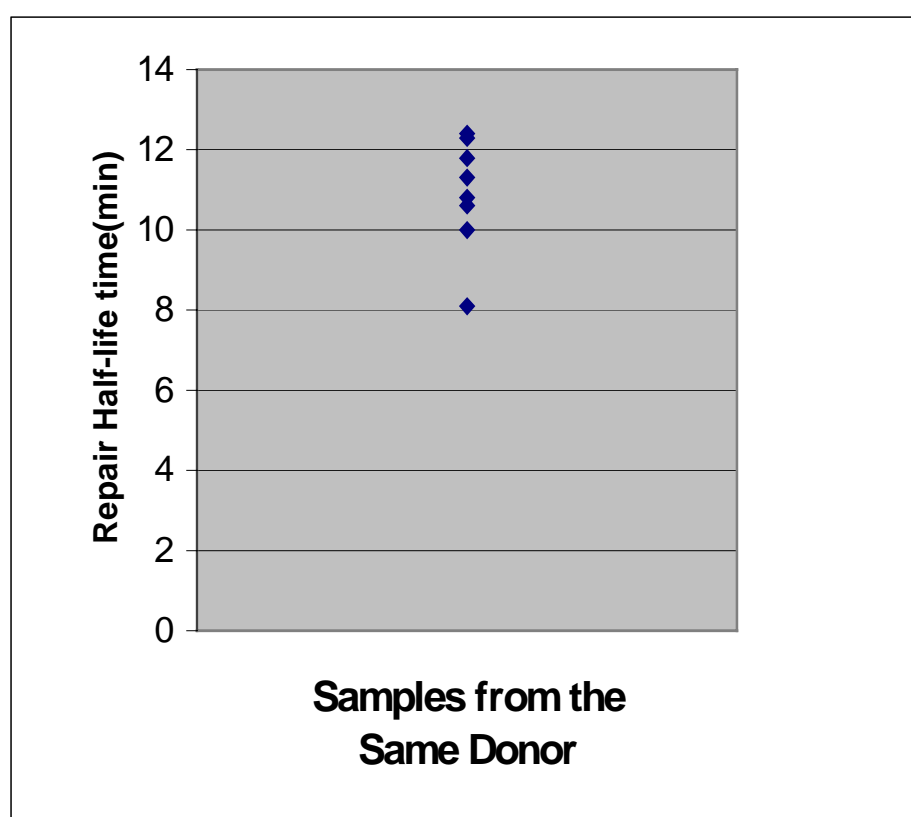


Fig. 22. *Determination of half-live times in eight independent DNA-repair assessments in mononuclear blood cells from the same human donor. Half-life times were determined by linear regression of the initial phase of repair as in Fig. 21. The average half-life time of this donor has been determined to be 10.9 min. The standard deviation was found to be 1.41 min (13%).*

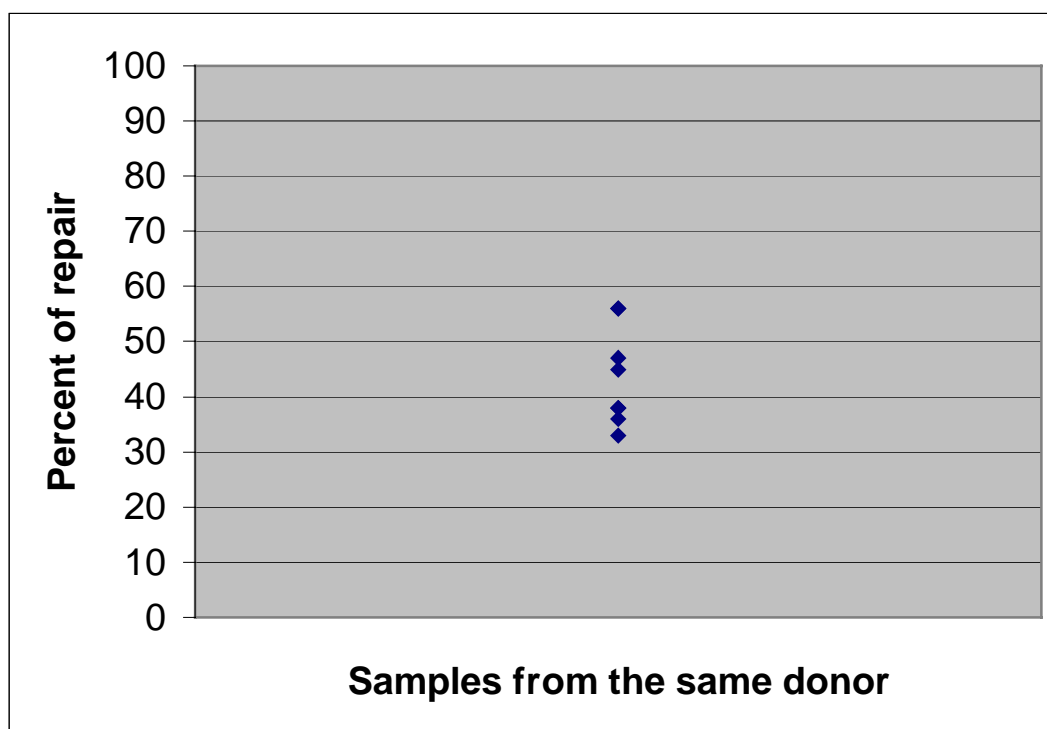


Fig. 23. Determination of percentage of repaired DNA in eight independent experiments on mononuclear blood cells of the same donor. The percentage of repaired DNA was determined by dividing the fraction of DNA repaired at 50 min (damage equivalent in Gy) by the initial damage introduced into the DNA in the damaging procedure. On average 44 % of the DNA damage was repaired. The standard deviation was found to be 10 % (i.e. 25% of the mean).

IV. 4. Comparison of DNA strand break repair in a long-lived (human) and a short-lived (rat) mammalian species.

In view of the known correlations of cellular stress resistance (Kapahi et al., 1999) and of cellular poly(ADP-ribosyl)ation capacity (Grube & Bürkle, 1992) with life span of mammalian species it was interesting to study if a similar correlation exists with DNA strand break repair following γ -irradiation. In the framework of the present thesis, such analysis was limited to a comparison of human (2 males and 4 females) and rat (2 males and 4 females) blood donors, for time constraints. The human donors were healthy volunteers 18 to 41 years old (*i.e.* not older than one third of the maximal human life span of 123 years), whereas the rats (strain Fischer 133) were 9 months old (*i.e.* one sixth of the maximal life span of 4.5 years). The isolated mononuclear cells were processed according to the standard protocol of

the automated FADU assay (Fig. 24. and Fig. 25.). The average repair half-life time of the human group was 10.35 min. The average half-life time of the rat group was 6.43 min (Fig.24). The difference in the half-life times of the two groups is statistically significant ($p = 0.001$ by T-test).

The average fraction of repaired DNA is 44 % in the human group compared with 17 % in the rat group (Fig. 25). The difference in the fraction of repaired DNA of the two groups is also statistically significant ($p = 0.001$ by T-test).

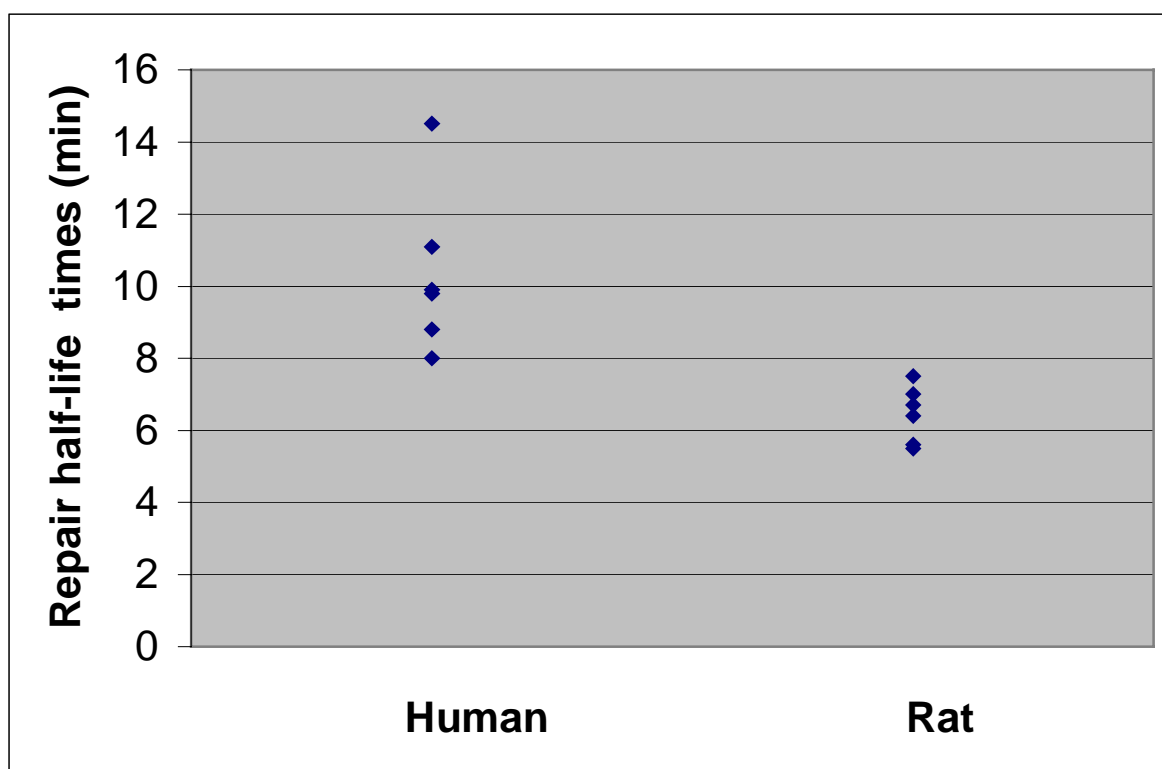


Fig. 24. Comparison of DNA repair half-life times in γ -irradiated mononuclear blood cells from rats and humans as measured by the automated FADU. Half-life times were determined by linear regression of the initial phase of repair as in Fig. 21. The average repair half-life time of the human group is 10.35 min. The average half-life time of the rat group is 6.43 min. The difference of the half-life times of the two groups is statistically significant ($p = 0.001$ by T-test)

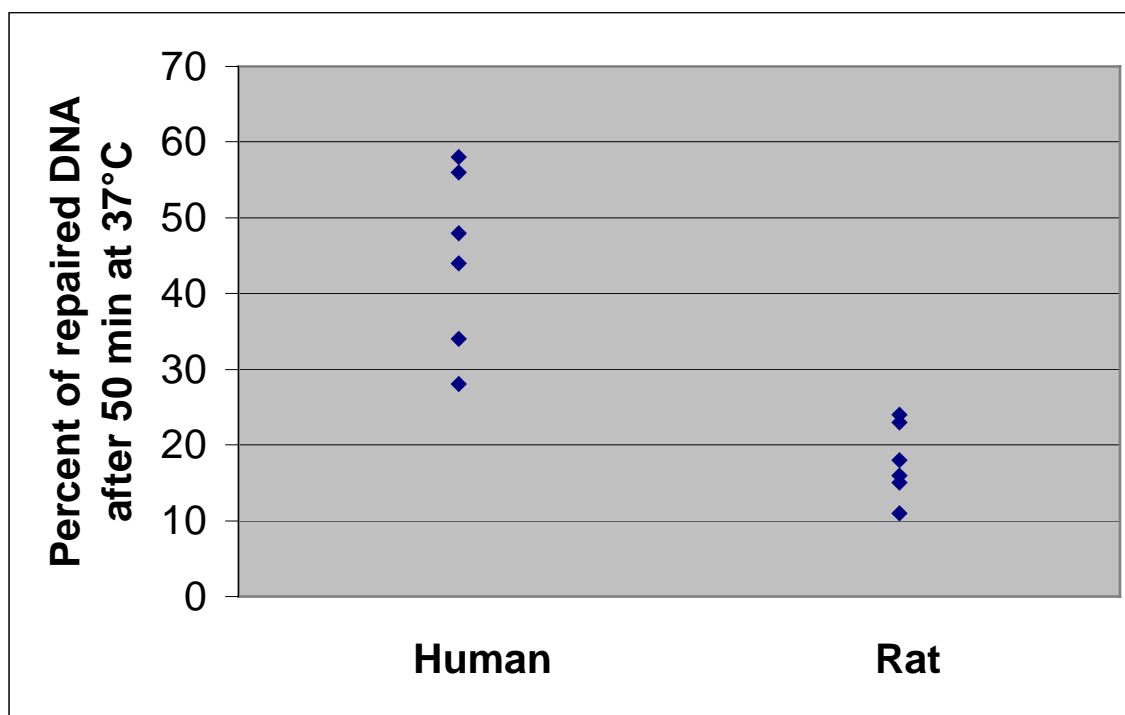


Fig.25. Comparison of percentage of repaired DNA in γ -irradiated mononuclear blood cells from rats and humans as measured by the automated FADU. The percentage of repaired DNA was determined by dividing the damage equivalent in Gy by reached at 50 min by the initial damage introduced into the DNA in the damaging procedure. The average of DNA repair is 44 % in the human group compared with only 17 % in the rat group. The difference of the half-life times of the two groups is statistically significant ($p = 0.001$ by T-test).

IV. 5. Comparison of DNA strand break repair in PARP-1^{-/-} and PARP-1^{+/+} cells.

PARP-1^{-/-} mice are known to be hypersensitive to whole-body γ -irradiation, dying from acute intestinal epithelial disturbances (Ménissier de Murcia et al., 1997). Therefore it was interesting to study DNA repair following γ -irradiation under cell culture conditions. Embryonic fibroblasts derived from PARP-1^{-/-} and PARP-1^{+/+} were trypsinised and then processed according to the standard automated FADU protocol. 2.7 Gy was applied as an initial damaging dose. In PARP-1^{+/+} cells 90 % the initial damage was repaired with a half-life time of 7 min. By contrasts, in PARP-1^{-/-} repair was below 15 % (Fig. 26). These data correspond very well to comet-assay data from de Murcia's group who have found that strand break resealing is impaired in PARP-1^{-/-} mouse fibroblasts after alkylation damage with methylmethanesulfonate (Trucco et al., 1998).

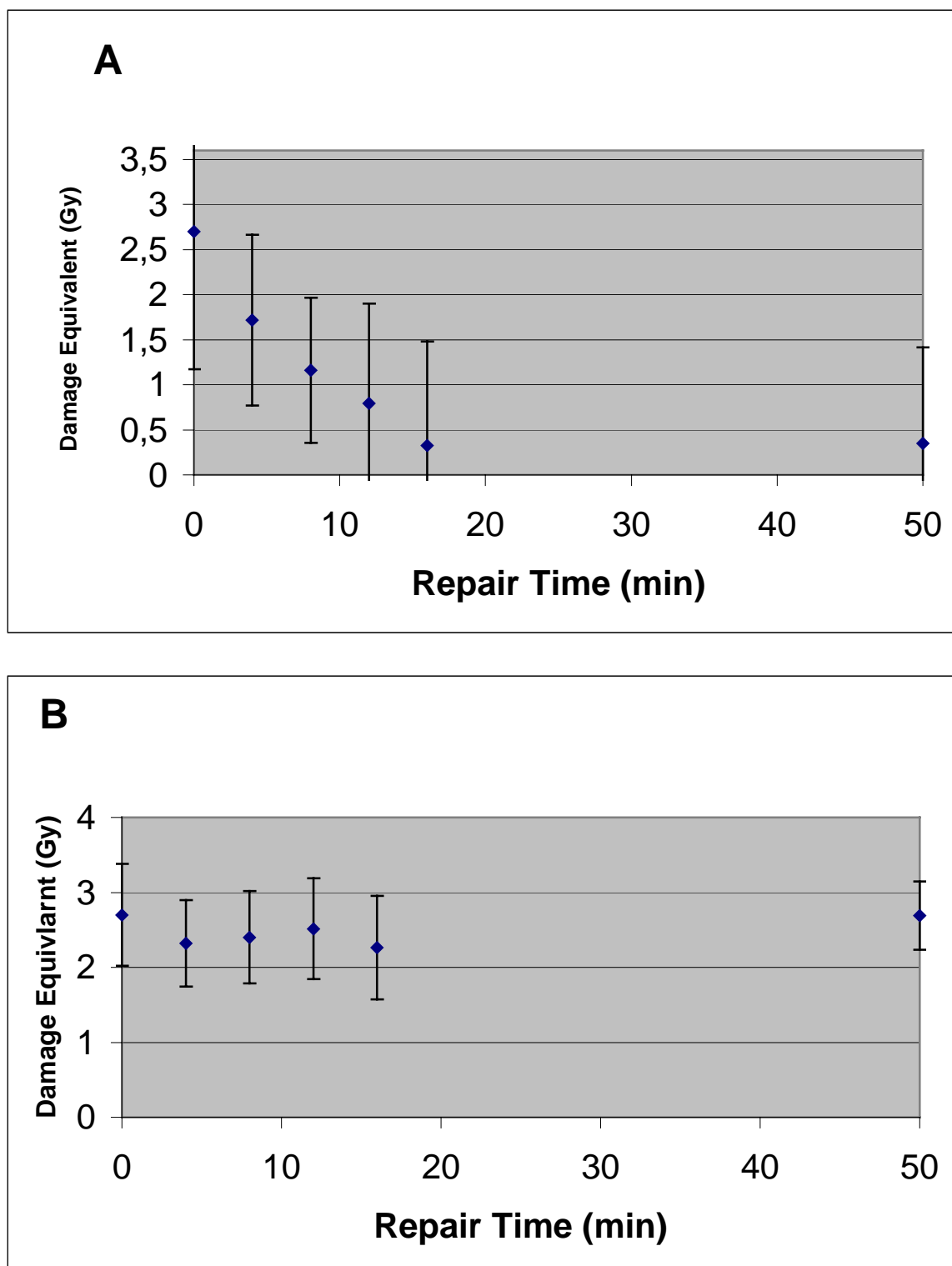


Fig. 26. DNA strand break repair after γ irradiation of $PARP-1^{-/-}$ and $PARP-1^{+/+}$ mouse embryonic fibroblasts. Repair was measured using the standard protocol for the automated FADU assay. In panel A $PARP-1^{+/+}$ and in panel B $PARP-1^{-/-}$ data are shown. Measurable repair is observed only in the wild-type ($PARP-1^{+/+}$) cells.

V. Discussion

The work presented in this thesis consists out of two main parts, *i.e.* the development of an immuno-dot-blot method to detect maximal poly(ADP-ribosyl)ation capacity in permeabilised cells, and the modification and automation of the FADU assay.

The activation of p(ADPr) formation is one of the fastest responses of the cell to genotoxic stress. It has been shown that PARP-1 is involved in the BER pathway, and apart from that seems to have many more functions in the cell (de Murcia & Shall 2000; Bürkle 2001). Maximal poly(ADP-ribosyl)ation capacity in permeabilised mononuclear blood cells was found to be positively correlated with life span of mammalian species (Grube and Bürkle, 1992). It has also been found that centenarian derived cells possess higher specific poly(ADP-ribosyl)ation capacity than controls (Muiras et al., 1998). These data have been obtained using the assay developed by Berger and colleagues (1979). The assay uses radioactively labelled NAD^+ . Major drawbacks to use this assay were the use of radioactivity, the relatively large cell numbers needed, and the poor reliability of washing steps to remove any unincorporated NAD^+ from TCA precipitates.

In the present theses a new, nonisotopic, simple method for the assessment of poly(ADP-ribosyl)ation capacity has been developed. Contrary to the initial expectation, the choice of a fairly large blotting area ($> 100 \text{ mm}^2$) proved essential, since the permeabilised cells tend to form clusters, which leads to heterogeneity and reduced precision. This clustering effect is averaged by using relatively large blotting areas. Commercially available 96-well manifolds have dotting areas of only 7 mm^2 , and thus are not suitable for this assay. Based on a commercially available 96-well manifold a 24-well manifold was manufactured with dotting areas of 113 mm^2 (12 mm diameter).

The applicability of the new immuno-dot-blot technique for the measurement of PARP inhibitor potency is highlighted by the successful confirmation of the IC_{50} value of the classical ADP-ribosylation inhibitor 3-aminobenzamide

Recently, Affar and colleagues (1998) described another immuno-dot-blot method to detect p(ADPr) synthesized in living cells or *in vitro*. However, an obligatory step in that method is the laborious purification of p(ADPr) by dihydroxyboronate chromatography before immunodetection can be performed. By contrast, the present method does not require any pre-purification.

In conclusion, the major advantages of the present method are the following: (a) Fewer than 100,000 cells per reaction are needed; (b) the assay is simple to perform and robust; (c) there

is no risk of interference by unincorporated NAD^+ , due to the excellent specificity of 10H monoclonal antibody (Kawamitsu et al., 1984; Bürkle et al., 1993).

Furthermore in an experiment comparing PARP-1^{+/+} with PARP-1^{-/-} cell lines it was possible to clearly demonstrate that the majority of polymer formation assessed in this assay is due to PARP-1 and not to PARP-2. This observation is very relevant, as it allows narrowing down previously obtained effects, such as correlation of cellular poly(ADP-ribosyl)ation capacity with longevity of species, to PARP-1, thus giving clear directions for further research along these lines.

At present PARP-1 is rapidly gaining interest in the fields of biogerontology and cancer research. Furthermore, PARP-1 has been implicated in a variety of highly prevalent and disabling human diseases, such diabetes type I, stroke and myocardial infarction (de Murcia & Shall, 2000; Bürkle, 2001b). Therefore the new assay may prove a useful tool for further elucidation of how PARP-1 is involved in each of these phenomena and may be especially well suited for clinical or population-based studies involving large numbers of samples to be tested functionally. Relevant questions to be addressed are the following: Can PARP-1 serve as a biomarker of ageing / longevity? Can PARP-1 serve as a marker of (organ-specific) cancer risk?

In mammals there are three main pathways for DNA repair: BER, NER and MMR. Damage produced by γ -radiation is mostly repaired by the BER pathway, whereas lesions derived from UV-B and UV-C are mostly repaired via NER. The most commonly used assay to measure DNA damage and DNA-excision repair is the comet assay. It has recently been improved but is still a very tedious procedure, as gels have to be prepared and to be processed manually in multi step protocols. As the original version of the FADU assay is also extremely laborious and very difficult to standardize, it is hardly used any more.

The automated and modified version of the FADU assay presented in this theses enables measurement of DNA strand breaks and DNA repair in a very convenient manner. The whole assay, including cell lysis and the alkali exposure leading to DNA unwinding, is carried out in a fully automated fashion by the robot, taking 2.5 h time. As the assay is performed in a 96-well format, multiple parallel determinations can easily be implemented, thus adding to the overall sensitivity and reliability of the assay. Only the readout and the preparation of the cells have to be done manually. Thus the workload has been dramatically reduced compared to the

original protocol by Birnboim & Jevcak. The cell number for a complete repair assay needed is 7 million, corresponding to approximately 5 ml of human blood.

In the automated FADU version, DNA damage induced by γ -radiation yields a linear dose response relationship between 0 and 2.7 Gy γ -radiation. Using shorter alkali incubation times higher doses could also be quantified. Repair can be efficiently measured following an initial damage of 2.7 Gy, thus using the linear range of the dose response curve. It should be noted that 2.7 Gy is a rather mild irradiation dose and therefore any data obtained should be of high physiological relevance. The very high reproducibility of the assay was highlighted by a series of 8 independent repair assays using blood from the same donor, yielding an average repair half life time of 10.9 min with a standard deviation of 1.41 min (13%).

Attempts to use standard commercial 96-well plates failed (data not shown), as the volume of the initial cell suspension and the volumes of all subsequent buffers proved too small to be delivered with the high level of accuracy required. Therefore the present format of the assay relies on a custom-made 96-well plate with deeper-than-standard wells (1 ml per well).

To ensure that all wells are held at precisely the same temperature a dedicated cooling device was set up to fully encase the 96-well plate. Cooling only from the bottom had turned out not to be sufficient. Further developments towards even higher levels precision and automation are currently ongoing. For instance the repair procedure could further be automated in such a way that samples would be placed on an integrated heating block and repair would be stopped by the robot diluting the cell suspension 1 in 10 and delivering the samples directly in the pre-cooled wells.

During the course of the work a multi-channel diluter was also tested, with the hope of cutting back total assay time by reducing time periods necessary for robot-operated dispensing. Unfortunately, however, use of the multi-channel diluter led to a loss of assay precision and therefore this option has since then not been pursued any further. Nevertheless, in view of subsequent changes made to the assay protocol, it might be worth re-considering use of a multi-channel diluter for certain special applications.

Another possible improvement that is currently under being developed is the robot-mediated delivery also of the Sybr green solution. However, this clearly will require availability of a

second diluter reserved for pipetting the Sybr green solution. Sybr green, being an intercalator, is an inhibitor of DNA unwinding. If the diluter or the reaction mixture were to be contaminated with traces of Sybr green early during the assay procedure, then predictably DNA unwinding would be severely disturbed and the assay would basically not work any more.

To address the question of whether capacity or half-life time of BER can be correlated with the lifespan of mammalian species an initial set of experiments was performed comparing mononuclear blood cells from 6 human and 6 rat donors. Surprisingly, the half life-time of the repair of the rats was found to be significantly shorter, with 6.3 min in rats as compared to 10.2 min in humans. However, the fraction of strand breaks repaired was significantly lower in the rat, with 17 % as compared to 45 % in the group of humans. This surprisingly clear result obtained with a very small number of probands is very encouraging, even if in the end it might not reflect a difference between the two species but a specific effect of the particular rat strain used, since no such rat strain-specific differences in BER have been reported so far.

To further investigate the effect of PARP-1 on the BER pathway repair experiments were performed comparing PARP-1^{+/+} and PARP-1^{-/-} mouse embryo fibroblast cells. In PARP-1^{+/+} cells 90 % of the initial damage was repaired with a half-life time of 7 min. By contrast, in PARP-1^{-/-} cells no clear evidence of any significant repair activity was observed. These dramatic results correspond very well to the data from de Murcia's group (Trucco, 1998) who have found that DNA repair is impaired in PARP-1^{-/-} fibroblasts exposed to alkylation treatment. The present data, relying on an alternative damaging procedure (γ -radiation), clearly underline the critical involvement of PARP-1 in the base excision repair pathway.

The above examples illustrate the usefulness of the automated FADU assay. This assay, like the poly(ADP-ribosyl)ation capacity assay discussed above, should be very suitable for further correlative studies in the field of ageing research. It could also be applied to address possible correlations of BER capacity with diseases like cancer or stroke or diabetes.

Apart from such uses, the quantitative assessment of exogenous DNA damage and also of DNA repair activities is of utmost importance not only for a broad range of basic scientific research fields but also for routine tasks, such as medical monitoring of patients or probands to assess individual genotoxic exposures and the body's response to them, as well as toxicological screening in the chemical and pharmaceutical industry or monitoring of environmental pollution. The present FADU assay can be expected to facilitate also research on, or routine monitoring of, exogenous genotoxic exposures.

VI. Summary

The work presented in this thesis consists of two main parts, *i.e.* (i) the development of a new immuno-dot-blot method to detect poly(ADP-ribosyl)ation capacity in permeabilised cells and (ii) the automation of the fluorescence detected alkaline DNA unwinding (FADU) assay to measure DNA strand breaks and repair.

The activation of poly(ADP-ribose) formation is one of the fastest responses of the cell to genotoxic stress. It has been shown that poly(ADP-ribose) polymerase-1 (PARP-1) is involved in DNA base-excision repair pathway and the maintenance of genomic stability in cells under genotoxic stress, but apart from this PARP-1 emerges to have many more functions in cellular physiology and pathophysiology. Interestingly, cellular poly(ADP-ribosyl)ation capacity is correlated with maximal life span in mammalian species and a high capacity is also associated with longevity in humans. Such data have been gained with an assay developed by Berger and colleagues, using radioactively labeled NAD^+ as a substrate. Major drawbacks of this assay were the use of radioactivity, the relatively large cell numbers needed, and the poor reliability of washing steps to remove any unincorporated NAD^+ from TCA precipitates.

In this thesis a new, non-isotopic, simple and reliable method for the assessment of poly(ADP-ribosyl)ation capacity is presented. Cells are prepared either by trypsination of monolayer cultures or by separating mononuclear blood cells using Percoll gradients. Cells are permeabilised and a reaction mixture containing unlabelled NAD^+ and an 'activator' oligonucleotide is added. The p(ADPr) formation reaction is stopped by addition of the ADP-ribosylation inhibitor 3-aminobenzamide. Cell ghosts are then dotted on a nylon membrane, precipitated *in situ* with TCA and washed with ethanol. As a first antibody monoclonal antibody 10H directed against the p(ADPr) is used. Peroxidase-coupled anti-mouse immunoglobulin serves as a second antibody. The chemoluminescence generated during the subsequent ECL+ reaction is captured and quantified using a chemoluminescence reader. In an dose-response experiment using the established poly(ADP-ribosyl)ation inhibitor 3-aminobenzamide an IC_{50} of 39 μM was found for this compound, corresponding very well with data from the literature and highlighting the usefulness of the assay. Furthermore, in experiments comparing fibroblasts derived from wild-type mice (PARP-1^{+/+}) with those from PARP-1 knockout mice (PARP-1^{-/-}) it was possible to demonstrate that the p(ADPr) formation assessed in this assay is due almost exclusively to PARP-1 and only in trace amounts to PARP-2 or other members of the PARP enzyme family.

The most commonly used assay to measure DNA damage and DNA-excision repair activity is the 'comet' assay. Despite recent improvements, this assay represents still a very tedious multi-step procedure, requiring well-trained operators and presenting extensive workload. Likewise, the originally published version of the FADU assay is very laborious and difficult to standardize.

In this thesis an automated simplified version is described. All steps necessary for cell lysis and DNA unwinding have been automated and the fluorescent readout is carried out using a 96-well fluorescence reader rather than single-cuvette format. Other aspects of the assay have also been optimised. For instance, the cell number has been cut down to 70,000 cell per data point, thus reducing the total number of cells required for a complete repair assay to less than 7 million.

The automated FADU assay is characterised by a very high level of reproducibility, as attested by repeated testing of fresh blood cells obtained from the same donor on consecutive days. Repair half-life times for cells from this human donor were on the average 10.9 min with a standard deviation of 1.41 min. On the average 45 % of the damage was found to be repaired, with a standard deviation of 7 %.

To investigate if DNA base-excision repair capacity or half-life time can be correlated with the life span of mammals an preliminary set of comparative experiments on γ -irradiated human and rat blood cells was performed. Surprisingly, the half life-time of the repair of the six rats tested was found to be significantly shorter than in the six human donors (6.3 min vs 10.2 min). By contrast, the percentage of lesions repaired during the first hour after irradiation was significantly lower in the rat cells (17% vs 45 %). Whether these findings relate to differences between species or reflect some rat strain-specific features remains to be clarified in future work.

To get some additional information about the involvement of PARP-1 in DNA base excision repair, experiments have been done comparing DNA strand break repair in PARP-1^{-/-} and in PARP-1^{+/+} fibroblasts after a damaging dose of 2.7 Gy. DNA repair was found to be dramatically impaired in PARP-1^{-/-} cells but very active in PARP-1^{+/+} cells. These results represent additional clear evidence for the involvement of PARP-1 in base excision repair.

VII. References

Affar EB, Duriez PJ, Shah RG, Sallmann FR, Bourassa S, Küpper JH, Bürkle A, Poirier GG (1998) Immunodot blot method for the detection of poly(ADP-ribose) synthesized in vitro and in vivo.

Anal. Biochem. 259: 280-283

Althaus F. R. and Richter C. (Eds.) (1987): ADP-ribosylation of proteins: Enzymology and biological significance.

Springer-Verlag, Berlin

Althaus F.R., Hofferer L., Kleczkowska H.E., Malanga M., Naegeli H., Panzeter P.L, Realini C.A. (1994) Histone shuttling by poly ADP-ribosylation.

Mol. Cell. Biochem. 138: 53-59

Alvarez-Gonzalez R, Spring H, Müller M, Bürkle A (1999) Selective loss of poly(ADP-ribose) and the 85-kDa fragment of poly(ADP-ribose) polymerase in nucleoli during alkylation-induced apoptosis of HeLa cells.

J Biol Chem 274: 32122-32126

Amé J.-C., Rolli V., Scheiber V., Niedergang C., Apiou F., Decker P., Muller S., Höger T., Ménissier-de Murcia J., and de Murcia G., (1999): PARP-2, a novel mammalian DNA-damage dependent poly(ADP-ribose) polymerase.

J. Biol. Chem. 274: 17860

Banasik, M., Komura, H., Shimoyama, M., and Ueda, K. (1992) Specific inhibitors of poly(ADP-ribose) synthetase and mono(ADP-ribosyl)transferase.

J. Biol. Chem. **267**, 1569–1575

Beneke S., Meyer R. and Bürkle A. (1997): Isolation of cDNA encoding full length rat (*Rattus norvegicus*) poly(ADP-ribose) polymerase

Biochem. Mol. Biol. Int. 43: 755 - 761

Beneke S, Alvarez-Gonzalez R, Bürkle A (2000) Comparative kinetic characterisation of baculovirus-expressed human and rat poly(ADP-ribose) polymerase-1.

Exp Gerontol 35: 989-1002

Berger N. A. (1985): Poly(ADP-ribose) in the cellular response to DNA damage.

Radiat. Res.101: 4 – 15

Berger NA, Sikorski GW, Petzold SJ, Kurohara KK. (1979) Association of poly(adenosine diphosphoribose) synthesis with DNA damage and repair in normal human lymphocytes. J

Clin Invest 63: 1164-1171

Birnboim HC, Jevcak JJ. (1981) Fluorometric method for rapid detection of DNA strand breaks in human white blood cells produced by low doses of radiation.

Cancer Res 41:1889-1892

Braun S. A., Panzeter P. L., Collinge M. A., Althaus F. R. (1994): Endoglycosidic cleavage of branched polymers by poly(ADP-ribose) glycohydrolase.

Eur. J. Biochem. 220: 369 - 375

Bürkle A (2001a) Poly(ADP-ribosyl)ation. *In*: M Schwab (ed), Cancer Research – an encyclopedic reference. Springer, Heidelberg, Germany

Bürkle A (2001b) Physiology and pathophysiology of poly(ADP-ribosyl)ation.

BioEssays, 23:795-806

Bürkle A (2001c) Poly(ADP-ribosyl)ation, a DNA damage-driven protein modification and regulator of genomic instability.

Cancer Lett, 163: 1-5

Bürkle A (2001d) Mechanisms of ageing.

Eye, 15: 371-375

Bürkle A (2001e) PARP-1: a regulator of genomic stability linked with mammalian longevity.

ChemBioChem, 2: 725-728

Bürkle A, Chen G, Küpper JH, Grube K, Zeller WJ (1993) Increased poly(ADP-ribosyl)ation in intact cells by cisplatin treatment.

Carcinogenesis (London) 14: 559-561

Bürkle A, Müller M, Wolf I, Küpper JH (1994) Poly(ADP-ribose) polymerase activity in intact or permeabilized leukocytes from mammalian species of different longevity.

Mol Cell Biochem 138: 85-90

Chambon P., Weill J. D., Doly J., Strosser M. T., Mandel P. (1966): On the formation of a novel adenylic compound by enzymatic extracts of the rat liver nuclei.

Biochem. Biophys. Res. Commun. 25: 638 - 643

Dantzer F., de la Rubia G., Ménissier-de Murcia J., Hostomsky Z., de Murcia G. and Schreiber V. (2000): Base excision repair is impaired in mammalian cells lacking poly(ADP-ribose) polymerase-1.

Biochemistry 39: 7559

Dianov G. L., Prasad R., Wilson S. H. and Bohr, V. A. (1999): Role of DNA polymerase- β in the excision step of long patch mammalian base excision repair.

J. Biol. Chem., 274: 13741

Dantzer F., Nasheuer H-P., Voensch J-L, de Murcia G., Ménissier-de Murcia J. (1998): Functional association of poly(ADP-ribose)polymerase with DNA polymerase α -primase complex: a link between DNA strand break detection and DNA replication.

Nucl. Acid Res. 26: 1891 - 1898

de Lange T., (1998): Length control of human telomeres.

Cancer J. Sci. Am., 4 (Suppl. 1), S22

de Murcia G., Huletsky A. and Poirier G. G. (1988): Modulation of chromatin structure by poly(ADP-ribosyl)ation.

Biochem. Cell Biol.66: 625

de Murcia G., Huletsky A., Lamarre D., Gaudereau A., Pouyet J., Daune M. and Poirier G. G. (1986): Modulation of chromatin superstructure induced by poly(ADP-ribose) synthesis and degradation.

J. Biol. Chem. 261: 7011

de Murcia G., Shall S. (Eds.) (2000): From DNA damage and stress signalling to cell death
Poly ADP-ribosylation reactions

Oxford university press

Durkacz B. W., Omidiji O., Gray D. A., Shall S. (1980): (ADP-ribose)_n participates in DNA excision repair.

Nature 283: 593 - 596

Eliasson M. J. L., Sampei K., Mandir A. S., Hurn P. D., Traystman R. J., Bao J., Pieper A., Wang Z.-Q., Dawson T. M., Snyder S. H., Dawson V. L. (1997): Poly(ADP-ribose) polymerase gene disruption renders mice resistant to cerebral ischemia.

Nat Med 3: 1089 - 1095

Giner H., Simonin F., de Murcia G., Menissier-de Murcia J. (1992): Overproduction and large-scale purification of the human poly(ADP-ribose) polymerase using a baculovirus expression system.

Gene 114: 279 - 283

Gradwohl G., Ménissier-de Murcia J., Molinete M., Simonin F., Koken M., Hoeijmakers J. H. J., de Murcia G. (1990): The second zinc-finger domain of poly(ADP-ribose) polymerase determines specificity for single-stranded breaks in DNA.

Proc. Natl. Acad. Sci. USA 87: 2990 - 2994

Grube K. and Bürkle A. (1992): Poly(ADP-ribose) polymerase activity in mononuclear leukocytes of 13 mammalian species correlates with species-specific life span.

Proc Natl Acad Sci USA 89: 11759-11763.

Grube K., Küpper J.H., Bürkle A. (1991) Direct stimulation of poly(ADP ribose) polymerase in permeabilized cells by double-stranded DNA oligomers.

Anal Biochem 193: 236-239

Harrington L., Mcphail T., Mar V., Zhou W., Oulton R., Bass M. B., Arruda I., Robinson M. O. (1997): A mammalian telomerase-associated protein.
Science 275: 973

Huppi K., Bhatia K., Siwarski D., Klinman D., Cherney B., Smulson M. (1989): Sequence and organization of the mouse poly(ADP-ribose) polymerase gene.
Nucl. Acid Res. 17: 3387 - 3401

Ikejima M., Noguchi S., Yamashita R., Suzuki H., Ogura T., Sugimura T., Gill D. M., Miwa M. (1990): The zinc-fingers of human poly(ADP-ribose) polymerase are differently required for the recognition of DNA breaks and nicks and the consequent enzyme activation.
J. Biol. Chem. 35: 21907 - 21913

Jacobson M. K., Payne, D. M., Alvarez- Gonzalez R., Juarez Salinas H., Sims J. L. and Jacobson E. L. (1984): Determination of in vivo levels of polymeric and monomeric ADP-ribose by fluorescence methods.
Meth. Enzymol. 106: 483 -494

Jean L., Risler J. L., Nagase T., Coulouarn C., Nomura N. and Salier J. P. (1999): The nuclear protein PH5P of the inter- α -inhibitor superfamily: a missing link between poly(ADP-ribose) polymerase and the inter- α -inhibitor family and a novel actor of DNA repair?
FEBS Lett., 446: 6.

Johansson M.(1999): A human poly(ADP-ribose)polymerase gene family (ADPRTL): cDNA cloning of two novel poly(ADP-ribose) polymerase homologues.
Genomics, 57: 442

Kapahi P, Boulton ME, Kirkwood TB (1999) Positive correlation between mammalian life span and cellular resistance to stress. Free Radic Biol Med 26:495-500

Kawamitsu H, Hoshino H, Okada H, Miwa M, Momoi H, Sugimura T (1984) Monoclonal antibodies to poly(adenosine diphosphate ribose) recognize different structures. *Biochemistry* 23: 3771-3777

Kickhoefer V. A., Siva A. C., Kedersha N. L., Inman E. M., Ruland C., Sreuli M., and Rome L. H. (1999): The 193-kD vault protein, VPARP, is a novel poly(ADP-ribose) polymerase. *J. Cell. Biol.* 146: 917

Kickhoefer V. A., Rajavel K. S., Scheffer G. L., Dalton W. S., Scheper R. J. and Rome L. H. (1998): Vaults are up-regulated in multidrug-resistant cancer cell lines *J. Biol. Chem.* 273: 8971

Kirkwood TB, Austad SN (2000) Why do we age? *Nature* 408: 233-238

Kirkwood TB. (2000) Evolution of ageing. *Nature* 270: 301-304

Klungland A. and Lindahl T. (1997): Second pathway for completion of human DNA base excision-repair: reconstruction with purified proteins and requirement for DNaseIV (FEN1). *EMBO J.*, 16: 3341

Kaufmann S. H., Desnoyers S., Ottaviano Y., Davidson N. E., Poirier G. G. (1993): Specific proteolytic cleavage of poly(ADP-ribose) polymerase: an early marker of chemotherapy induced apoptosis. *Cancer Res.* 53: 3979 - 3985

LeCam E., Fack F., Menissier-de Murcia J., Cagnet J. A. H., Barbin A., Sarantoglou V., Revet B., Delain E., de Murcia G. (1994): Conformational analysis of a 139 base-pair DNA containing a single-stranded break and its interaction with human poly(ADP-ribose)polymerase. *J. Mol. Biol.* 235: 1062 - 1071

Ludwig A., Behnke B., Holtlund J., Hilz H. (1988): Immunoquantification and size determination of intrinsic poly(ADP-ribose) polymerase from acid precipitates. An analysis of the in vivo status in mammalian species and lower eucaryotes. *J. Biol. Chem.* 263: 6993 - 6999

Mendoza-Alvarez H. and Alvarez-Gonzalez R. (1993): Poly(ADP-ribose)polymerase is a catalytic dimer and the automodification reaction is intermolecular.

J. Biol. Chem. 268: 22575 - 22580

Ménissier de Murcia J, Niedergang C, Trucco C, Ricoul M, Dutrillaux B, Mark M, Oliver FJ, Masson M, Dierich A, LeMeur M, Walztinger C, Chambon P, de Murcia G. (1997)

Requirement of poly(ADP-ribose) polymerase in recovery from DNA damage in mice and in cells.

Proc Natl Acad Sci USA 94: 7303-7307

Meyer R., Müller M., Beneke S., Küpper J.-H., Bürkle A. (2000): Negative regulation of alkylation-induced sister-chromatid exchange by poly(ADP-ribose) polymerase-1 activity. .

Int J Cancer. 88: 351-355.

Muiras M.-L., Müller M., Schächter F., Bürkle A. (1998): Increased poly(ADP-ribose) polymerase activity in lymphoblastoid cell lines from centenarians.

J. Mol. Chem. 264: 14382 - 14385

Naegleli H. and Althaus F. R. (1991): Regulation of poly(ADP-ribose) polymerase. Histone specific adaptations of reaction products.

J. Biol. Chem. 266: 10596 - 10601

Pero R. W., Holgren K., Persson L. (1985): Gamma-radiation induced ADP-ribosyl transferase activity and mammalian longevity.

Mutat. Res. 142: 69 - 73

Radons J., Heller B., Bürkle A., Hartmann B., Rodriguez M. L., Kroncke K. D., Burkart V., Kolb H. (1994): Nitric oxide toxicity in islet cells involves poly(ADP-ribose) polymerase activation and concomitant NAD⁺ depletion.

Eur. J. Biochem. 220: 369 - 375

Saito I., Hatakeyama K., Kido T., Ohkubo H., Nakanishi S., Ueda K. (1990): Cloning of a full-length cDNA encoding bovine thymus poly(ADP-ribose) synthetase: evolutionarily conserved segments and their potential functions.

Gene 90: 249 - 254

Satoh M. S. and Lindahl T. (1992): Role of poly(ADP-ribose) formation in DNA repair.

Nature 356 - 358

Schlicker A, Peschke P, Bürkle A, Hahn EW, Kim JW (1999) 4-Amino-1,8-naphthalimide: a novel inhibitor of poly(ADP-ribose) polymerase and radiation sensitizer.

Int J Radiat Biol 75: 791-100

Seker H, Bertram B, Bürkle A, Kaina B, Pohl J, Koepsell H, Wießler M (2000) Mechanistic aspects of the cytotoxicity of glufosfamide a new tumour therapeutic agent.

Br J Cancer 82: 629-634

Shieh W. M., Amé J. C., Wilson M. V., Wang Z. Q., Koh D. W., Jacobson M. K.; Jacobson E. L. (1998): Poly(ADP-ribose)polymerase null mice synthesize ADP-ribose polymers.

J. Biol. Chem. 273: 30069 - 30072

Trucco C., Oliver F. J., de Murcia G., Ménissier-de Murcia J. (1998): DNA repair defect in poly(ADP-ribose) polymerase-deficient cell lines.

Nucl. Acids Res. 26: 2644

van Gool L., Meyer R., Tobiasch E., Cziepluch C., Jauniaux J-C., Mincheva A., Lichter P., Poirier G. G., Bürkle A., Küpper J-H. (1997): Overexpression of human poly(ADP-ribose) polymerase in transfected hamster cells leads to increased poly(ADP-ribosyl)ation and cellular sensitization to γ -radiation.

Eur. J. Biochem. 244: 15 - 20

van Stensel B. and de Lange T.(1997): Control of telomere length by the human telomeric protein TRF1.

Nature 385: 740

VIII. Own publications

Pfeiffer, R., Brabeck, C., and Bürkle, A. (1999). Quantitative nonisotopic immuno-dot-blot method for the assessment of cellular poly(ADP-ribosyl)ation capacity. *Anal. Biochem.* 275, 118-122.

Posters:

Pfeiffer, R., Brabeck, C., and Bürkle, A. A Rapid quantitative nonisotopic immuno-dotblot method for the assessment of poly(ADP-ribosyl)ation capacity of permeabilized cells. 40. Frühjahrstagung der DGPT, Mainz, March 9-11, 1999.

Pfeiffer, R., Brabeck, C., and Bürkle, A. A Rapid quantitative nonisotopic immuno-dotblot method for the assessment of poly(ADP-ribosyl)ation capacity of permeabilized cells. 10th AEK-Symposium. Heidelberg, March 24-26, 1999.

Pfeiffer, R., Brabeck, C., and Bürkle, A. A Rapid quantitative nonisotopic immuno-dotblot method for the assessment of poly(ADP-ribosyl)ation capacity of permeabilized cells. EMBO Workshop on molecular and cellular gerontology. Serpiano, Switzerland, 18-22 September 1999.

Pfeiffer R, Müller M, Bürkle A Improved Automated Version of the Fluorescence-Detected Alkaline DNA-Unwinding (FADU) Assay to Measure DNA Strand Breaks and DNA Repair 11th Congress of the Division of Experimental Cancer Research (AEK) of the German Cancer Society, Heidelberg, 4-6 April 2001

Pfeiffer R, Müller M, Bürkle A Improved Automated Version of the Fluorescence-Detected Alkaline DNA-Unwinding (FADU) Assay to Measure DNA Strand Breaks and DNA Repair; 13th International Symposium on ADP-Ribosylation, New York, NY, USA, 8-11 June 2001

Oral presentation at international conference:Ragen Pfeiffer; Methodology to assess DNA strand breaks and cellular poly(ADP-ribosyl)ation capacity;
Biogerontology Research Symposium, Horton Grange, Northumberland, UK, 21- 23 June
2001

IX. Acknowledgements

First and foremost, I would like to thank Dr. Alexander Bürkle who raised my interest in the subject matter, discussed this work and provided lots of helpful advice and encouragement on a day-to-day basis over the last few years.

I also express my gratitude to Professor Dr. Manfred Wießler for his willingness to supervise my PhD thesis and act as First Examiner at the Fakultät für Pharmazie, Ruprecht-Karls-Universität Heidelberg.

I would like to thank Professor Dr. Fricker and Professor Dr. Wink for their kind willingness to function as examiners of my PhD thesis

I also thank Professor Tom Kirkwood for his very welcoming reception in the Department of Gerontology and all the support and encouragement he gave me during my affiliation with the Department.

Further, I should like to thank Mr Marcus Müller, Mr Alan Leake and Mr Alexander Keith for valuable technical support and Mr Wolfgang Weinig for oligonucleotide synthesis.

I should like to express my special thanks to my parents who enabled and supported my studies.

Last not least, my thanks go to all former and current members of the lab for the help and the good atmosphere.

I should like to thank the companies Polygen GmbH (director: Mr Roland Friedberger) and Tecan GmbH Deutschland (director: Mr Martin von Lüder) for giving access to hardware components in the framework of a co-operation project.

Finally I thank the Bundesministerium für Bildung und Forschung (BMBF), Bonn, for financial support (BioRegio programme; grant to Dr A Bürkle, No 0311692/5).